TI 2018-100/IV
Tinbergen Institute Discussion Paper

Do information contagion and business model similarities explain bank credit risk commonalities?

Dieter Wang[1,2]
Iman (I.P.P.) van Lelyveld[1,2]
Julia (J.) Schaumburg[1]

[1] VU Amsterdam, The Netherlands
[2] De Nederlandsche Bank, The Netherlands

Do information contagion and business model similarities explain bank credit risk commonalities?*

Dieter Wang[a,b], Iman van Lelyveld[a,b], and Julia Schaumburg[a]

[a] *VU Amsterdam, Tinbergen Institute*
[b] *De Nederlandsche Bank*

December 2018

Abstract

This paper revisits the credit spread puzzle in bank CDS spreads from the perspective of information contagion. The puzzle, first detected in corporate bonds, consists of two stylized facts: Structural determinants of credit risk not only have low explanatory power but also fail to capture common factors in the residuals (Collin-Dufresne et al., 2001). For the case of banks, we hypothesize that the puzzle exists because of omitted network effects. We therefore extend the structural models to account for information spillovers based on bank business model similarities. To capture this channel, we propose and construct a new intuitive measure for portfolio overlap using the complete asset holdings of the largest banks in the Eurozone. Incorporating the network information into the structural model for bank credit spreads increases explanatory power and removes a systemic common factor as well as a North-South common factor from the residuals. Furthermore, neglecting the network likely overstates the importance of structural determinants.

Keywords: Information contagion, credit spread puzzle, bank business model similarities, portfolio overlap measure, dynamic network effects model.

JEL classifications: G01, G21, C32, C33, C38.

*The views expressed in this paper are those of the authors and do not necessarily represent the views of De Nederlandsche Bank. Comments from Christoph Aymanns, Fernando Duarte, Co-Pierre Georg, Paul Glasserman, André Lucas, Albert Menkveld, Mark Paddrik, Sriram Rajan, Bernd Schwaab, Miguel Segoviano, Sweder van Wijnbergen, Filip Zikes have greatly improved the paper. We are also grateful for comments and suggestions from participants and discussants at the 2017 Australasian Finance & Banking Conference, the 2017 IFABS, the 2017 IAAE, the 2017 SoFiE, the 2017 Spatial Econometrics Association conference, the 2017 Workshop on spatial and spatio-temporal data analysis, Tohoku University, the 2018 Econometric Society (EEA-ESEM), the 2018 IBEFA/WEAI, the 2018 RiskLab/Bank of Finland/ESRB Conference on Systemic Risk Analytics, and seminars at DNB, the Federal Reserve Board, the International Monetary Fund (MCM), and the Office of Financial Research. Schaumburg also thanks the Dutch Science Foundation (NWO, grant VENI451-15-022) for financial support. All remaining errors are ours. Corresponding address: DNB, PO Box 98, Westeinde 1, 1000AB, Amsterdam. Email: d.wang@vu.nl.

1 Introduction

In this paper, we show that similarities between bank business models constitute an important determinant of how markets value bank default risks. Market participants adjust their credit risk exposures to distressed banks using instruments such as credit default swaps (CDS). A bank's CDS price, therefore, reflects its default risk as it is perceived on the secondary market. In the empirical asset pricing literature, the credit spreads of corporates or banks are mainly modeled using company fundamentals and other structural variables, such as equity returns, the risk-free rate, or the slope of the yield curve. However, the seminal paper by Collin-Dufresne et al. (2001) and the subsequent empirical work of Bharath and Shumway (2008); Campbell and Taksler (2003); Ericsson et al. (2009); Fontana and Scheicher (2016); Zhang et al. (2009) show that these variables have low explanatory power and leave a systematic common factor unexplained. The lackluster explanatory power of variables grounded in economic theory is commonly referred to as the *credit spread puzzle*. We find the same puzzle in the CDS spread changes of the 22 largest banks in the Eurozone. Surprisingly, in addition to the systematic common factor, we also detect a North-South factor, that distinguishes between the Northern countries (Austria, Belgium, France, Germany and Netherlands) and Southern countries (Italy and Spain).

As the 2008 great financial crisis has painfully demonstrated, a bank's financial health may strongly depend on the health other banks. We therefore augment the structural regression model with network effects that capture information contagion about the creditworthiness of banks. Information contagion happens if one bank's CDS spread changes can be attributed to changes in another bank's spread, rather than to its own credit determinants. How informative and relevant one bank's CDS dynamics are for other banks depends on how similar the market perceives their business models to be. To measure business model similarity between banks, we propose a novel method for constructing portfolio overlap networks based on their complete asset holdings. We apply this overlap measure to the complete asset holdings of the largest banks in the Eurozone, comprising more than 240,000 unique ISINs from the quarterly reported Securities Holdings Statistics (SHS). These data are highly confidential and our analysis is currently only the second paper cleared for publication. Applying on our new overlap measure, we construct a portfolio overlap network in which the banks are the network's while the degree of portfolio overlap between any two banks is represented by the edges. The higher the overlap, the more similar the bank business models and the stronger the potential for information spillovers.

Embedding this network into the regression allows us to capture and distinguish between two types of effects: *structural network effects*, which take place if one bank's CDS changes are affected by shocks to a neighboring bank's structural credit determinants; and *residual network effects*, which capture the correlation structure among the idiosyncratic shocks of individual banks. These effects directly address the two stylized facts of the credit spread puzzle. First, structural network effects increase the average share of explained variance by up

to 15%. Second, the residual network effects halve the importance of the systematic common factor and remove its across-the-board nature, while also stripping the dividing characteristic off the North-South factor. At the same time, the coefficients of structural regressors also lose statistical and economic significance. These findings indicate that neglecting network effects likely overstates the importance of structural regressors in the extant literature. Although the dynamic nature of the DNE model leads to the best performance, most of its benefits can already be garnered by using constant network effects only.

Bank networks and information contagion

After the 2008 crisis, the systemic risk literature studied credit risk with networks and financial contagion occupying center stage (Glasserman and Peyton Young, 2015). This literature stresses that banks are part of an interconnected network where risks can cascade throughout the system. Banks thus cannot be analyzed in isolation; rather, they must be understood in relation to other banks. To identify a bank's peer group, the type of contagion mechanism at play must be taken into account. For instance, Allen and Gale (2000) model the direct lending exposure between banks wherein the lending relationships determine relevancy. In such cases, a bank's default risk depends on the banks it has loaned money to. If the borrowing banks face liquidity problems, these problems will ultimately impact the lender. If the lender, in turn, has also borrowed money from other banks, the process continues up the chain. In comparison, banks with common asset holdings become the relevant set when contagion is driven by fire-sales. In Cifuentes et al. (2005), banks facing sudden liquidity needs sell illiquid assets to satisfy capital requirements. The resulting downward price pressure can impact other banks with the same illiquid asset on their books, triggering another round of asset sales, and so on. Duarte and Eisenbach (2018) assess the vulnerability of a bank based on its share of holdings in illiquid, systemic assets. They isolate fire-sale spillovers as the cross-sectional aspect of aggregate vulnerability. This is consistent with the fire-sale framework of Greenwood et al. (2015), who provide an empirical approach to study the indirect vulnerability of banks following the deleveraging of other banks.[1]

To understand the credit risk contained in bank CDS spreads, we argue that structural credit spread models need to account for information contagion. In contrast to the mechanisms discussed above, this type of contagion is based on perception and beliefs. In terms of Brunnermeier et al's (2013) distinction between rational and psychological channels of contagion, our channel belongs to the latter. That is, the market's view on a bank's creditworthiness not only depends on its own fundamentals; it also depends on the creditworthiness of other banks with similar business models, i.e. its peers. A rise in a bank's CDS premium could therefore be attributed to an earlier CDS premium increase of another bank, which the market deems to be similar enough to be relevant. The underlying assumption is that news containing signals about one bank's financial health may not only be informative about that bank's default risk;

[1] Other notable contributions to the empirical literature on risk arising from bank interconnections include, for instance, Billio et al. (2012), Blasques et al. (2018), Demirer et al. (2018), and Hautsch et al. (2015).

the signal may also lead to the reassessment of another bank's credit risk, which we interpret as *information spillover*. The systemic risk literature studies information contagion from several aspects. Acharya and Yorulmazer (2008) demonstrate how, when a systematic common factor exists in loan returns because of investments in similar industries, bad news about one bank can be informative of the common factor and, in turn, lead to the higher borrowing costs of another bank. If the common factor is less prevalent, then the costs can increase even more because the signal is more informative, incentivizing banks to herd and invest in similar industries. This argument becomes one justification for Ahnert and Georg (2018), who also find that bad news about one bank can be informative about another bank with common exposures, leading to higher overall systemic risk. The authors furthermore justify this type of information spillover based on interbank lending, which we previously discussed under direct contagion. The type of information contagion we analyze in credit risk follows a similar rationale.

Deutsche Bank example The Deutsche Bank case clearly illustrates how bad news about one bank's financial health spills over to other banks, which, in turn, destabilizes the entire system. On January 20, 2016, Deutsche Bank issued a warning that it would not achieve its profit targets and that it recorded its first loss since 2008. In the following days, Deutsche Bank's CDS spreads rose rapidly, and many other large European banks followed suit. This overall increase of CDS premia reflected the growing concern by investors over the health of European banks (Kiewiet et al., 2017). These coinciding adjustments in market perceptions are likely driven by information spillovers, as European banks did not undergo any fundamental changes that would have warranted the volatile price movements. Furthermore, Deutsche Bank's CDS premium peaked *simultaneously* on February 11, 2016 with 14 other major banks. The buildup period and the synchronicity of peaks indicate that information cascades happened gradually over time.

Finding peers with portfolio overlaps

How vulnerable bank CDS contracts are to each other's signals, or how relevant their signals are for each other's repricing on the secondary market, depends on how similar the market regards their business model to be. For instance, if a German savings bank runs into financial trouble, the market is more likely to reassess the creditworthiness of other German savings banks in response, rather than that of Spanish corporate-oriented banks. Information contagion therefore depends on bank business model similarity. Identifying bank business models, therefore, has been an important goal of both supervisors and academics. A recent study by Cernov and Urbano (2018) highlights the importance of measuring these similarities for financial stability. These measures are crucial for assessing an institution's riskiness with respect to its peers, and for studying the possible impact of new regulations. Methods to group bank business models either rely on quantitative clustering methods, such as k-nearest neighbors, or on qualitative assessments based on bank activities, legal structures, or expert knowledge.

For our purpose of understanding information contagion in credit risk, we propose a novel method for quantifying business model similarities through portfolio overlaps. Because they have made similar investment, lending, or funding decisions in the past, banks that follow similar business models usually share similar balance sheet structures (Roengpitya et al., 2014, 2017). For instance, banks adapt their overall strategies and balance sheets to comply with new regulatory environments (Cernov and Urbano, 2018). Similarly, the fire-sale literature studies the implications of the link between asset holdings and business model strategies. Coval and Stafford (2007) argue that investors following similar strategies end up with portfolios that are concentrated in similar securities. Thus, they explain, if a bank liquidates its assets in a fire-sale then other banks with similar asset exposures will likely be affected. More importantly, we argue that there is a high likelihood for them to raise liquidity in the same manner, due to the similar strategies. Hence, only strategy-outsiders are able to absorb these shocks (Shleifer and Vishny, 1992). In sum, if two banks share almost identical asset holdings, we can use this similarity as an indicator for similar business models.

Modeling network effects

With knowledge of the underlying overlap network, we return to the original task of finding a potential answer to the credit spread puzzle. Our econometric model extends the structural regression model of Collin-Dufresne et al. (2001) with network effects. The main difference is that we do not only regress a bank's CDS changes on structural variables; we also regress on a weighted average of CDS changes of all other banks in the system. The weights correspond to the portfolio overlaps a bank has with all other banks. A scalar parameter in the unit interval determines the importance of these added network effects. We interpret this parameter as network intensity. If the intensity is zero, the model reverts back to Collin-Dufresne et al.'s structural regression model where CDS prices are independent of each other. Otherwise, information contagion takes place and CDS prices become functions of one another, depending their similarities. This functional dependency holds for all CDS contracts, such that negative beliefs can spillover from bank to bank. To ensure that this spillover process converges, we assume that its effect attenuates with each round. The speed of convergence is determined by the network intensity parameter.

In the model, we represent these rounds as successive linear transformations with the portfolio overlap network as the transformation matrix.[2] This iterative nature imitates the learning or price discovery process studied in the financial literature, where traders act under bounded rationality and imperfect knowledge. Most relevant to our work, Routledge (1999) shows how information diffusion based on adaptive or evolutionary learning across multiple periods can lead to a Grossman and Stiglitz (1980) type rational equilibrium. The success of this process crucially relies on the monotonic selection dynamic, where traders imitate better strategies

[2]This transformation matrix can be understood in the same manner as the input-output matrix from the Leontief model. Instead of sectors producing goods by combining goods from other sectors, our outputs are CDS prices resulting from the weighted combinations of other CDS prices.

more frequently than bad ones. Viewing the financial market as a complex system, Hommes (2008) studies bounded rational traders that improve their strategies either with adaptive learning or evolutionary selection. Using a simple cobweb model, he shows that the market price can converge to the rational expectations equilibrium in both cases.

The remainder of this paper is structured as follows. We first introduce the portfolio overlap measure, in Section 2, and then derive a Network Effects (NE) model and the Dynamic Network Effects (DNE) model based on a structural regression model in Section 3. Section 4 describes the data and Section 5 presents the empirical results before we conclude.

2 Portfolio overlap

The systemic risk literature has extensively studied portfolio overlaps and common asset exposures, especially in the context of fire-sales. While portfolio overlaps are key in our model, their main purpose is to model information contagion, not to capture actual fire-sales. However, if the market believes that one bank is vulnerable to another bank's rapid deleveraging efforts, then this belief would again constitute information contagion. The systemic risk literature is therefore closely related and highly relevant. For instance, Wagener (2010) highlights that, although portfolio diversification is desirable for individual institutions, it is dangerous on a macro level as it increases portfolio overlaps among banks and therefore exposes them to the same risks. Similarly, Caccioli et al. (2014) study a network model with overlapping portfolios and leverage. In their model, a system may become unstable if a critical threshold for leverage is crossed, resulting in system-wide contagion. Finally, Cont and Schaanning (2018) use portfolio overlaps to quantify a bank's mark-to-market losses resulting from the deleveraging decisions of another bank. Other studies provide empirical models that can be used for stress-tests. Greenwood et al. (2015), for example, study how banks that are seemingly unrelated can contaminate other banks because of indirect vulnerabilities to deleveraging externalities. They estimate their model with balance sheet data from the European Banking Authority. Poledna et al. (2018) also contribute to stress-testing by proposing a new systemic risk measure that relies on portfolio overlaps, which they calculate using the complete security holdings of major Mexican banks.

We develop a regression-based overlap measure that quantifies partial correlations between portfolio structures.[3] Intuitively, our measure asks how much the knowledge of one bank's portfolio helps in predicting the contents of another bank's portfolio, relative to all remaining banks. For instance, the measure would assign a high overlap between two German Landesbanken and a low overlap between a Landesbank and some other bank type. The outcome for the measure is because the holdings of one Landesbank is likely to be much more predictive of

[3]These correlations do not refer to correlations between the portfolios returns. Instead, we are interested in how similar portfolios are in structure. Thus, we treat portfolios as random vectors and the quantities held in each asset as a random variables. We then calculate the partial correlations within a set of portfolios or random vectors.

another Landesbank's holdings, compared to banks that follow an entirely different business model. Our proposed measure has three distinct properties:

Property 1: Non-negativity. The measure is either zero when banks have no assets in common, or positive if they share at least one asset. A negative overlap has no economic interpretation.

Property 2: Relativity. The measure varies with banks and assets in the system. A bank with high overlaps with all other banks may lose its central position once we include new banks and/or new assets.

Property 3: Asymmetry. If a bank holds a portfolio and all other banks only hold partitions thereof, then that bank can have a larger overlap with regards to one of the other banks than vice versa.

We define the overlap measure $\mu_{i,j}$ between banks i and j for a system $B = \{bank_1, ..., bank_N\}$. Each $bank_i$ holds a portfolio of assets that is represented by a random vector in an L-dimensional asset space. In the remainder of this section we derive the overlap measure. We start with the overlap between two banks and extend the concept for N banks.

Figure 1: Hypothetical financial sector with four banks

Left: A hypothetical financial system with four banks and 30 assets. Each column represents a bank portfolio and the blue bars indicate the amount a banks holds of a certain asset. Right: The portfolio overlap matrix W that results from applying Algorithm 1 to the asset holdings on the left panel. We can see that the W is asymmetric and row-normalized.

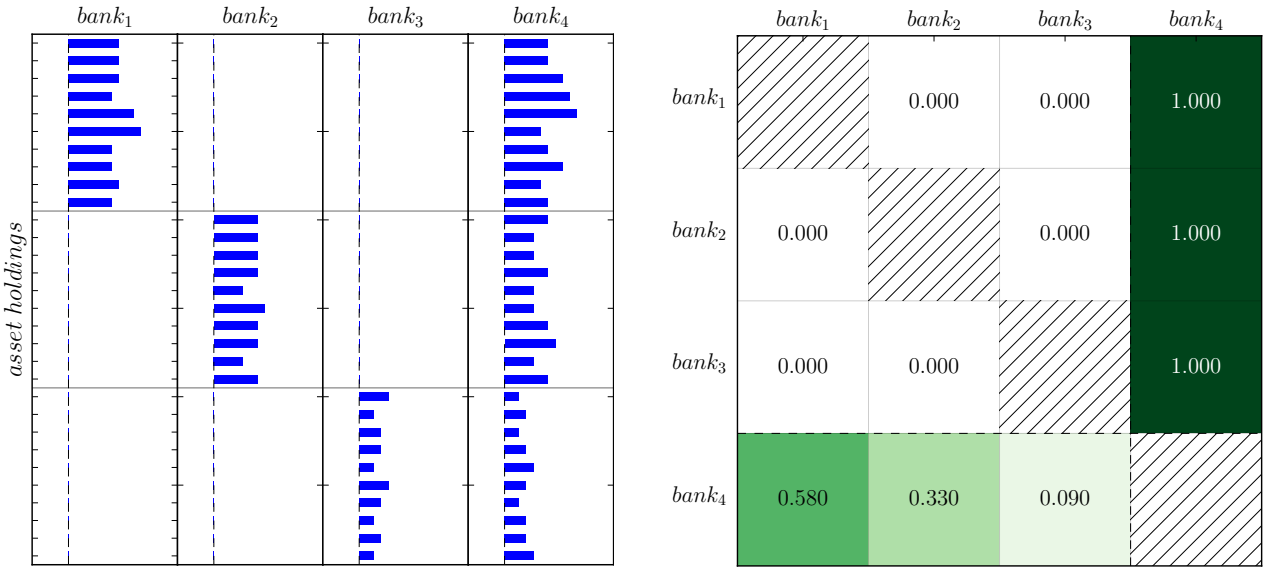

2.1 Derivation

It is instructive to begin with a system with two banks $B = \{bank_i, bank_j\}$. An obvious candidate for the overlap measure is the correlation coefficient between both vectors of observed holdings, $\mu_{i,j} = \rho_{i,j} = \text{corr}(bank_i, bank_j)$. Although this choice is intuitive and simple, it can violate the desirable non-negativity property.[4] As a remedy, we take the squared correlation coefficient. This is, in fact, the R^2 from a simple regression of $bank_i$ on $bank_j$ with no constant. The overlap measure is then $\mu_{i,j} = \rho^2_{i,j} = R^2$, which is, by definition, always non-negative.

$$bank_i = bank_j\beta + u_i.$$

In a general system with N banks $B = \{bank_1, ..., bank_N\}$, a natural extension is to calculate $\mu_{i,j}$ for all i and j pairs. However, this approach results in symmetric overlap measures, that is $\mu_{i,j} = \mu_{j,i}$. But symmetry is not desirable if the ultimate purpose of the measure is to capture information contagion among banks. To illustrate, consider the hypothetical system with four banks in Figure 1, left panel. For this illustration, we abstract from the effects of exogenous credit spread determinants. If we observe a drop of $bank_1$'s credit spread, then this drop can only be due to information spillover from $bank_4$. At the same time, if we observe a deterioration of $bank_4$'s creditworthiness, this information spillover can be partly ascribed to each of the other three banks. Symmetry would imply that both cases are informationally equivalent, which is not the case. For a more concrete example for why symmetry is undesirable, recall that perceived vulnerability to fire-sales also constitutes a type of information contagion. Clearly, $bank_4$ is most central as its portfolio shares common assets with all other banks while the other banks' portfolios only hold partitions of $bank_4$. If $bank_4$ suddenly needs to raise money, it could be a knock-on effect from either of the other banks liquidating their assets in a fire-sale. Conversely, if one of the other banks has to liquidate its assets, this portfolio adjustment can only be due to deleveraging efforts of $bank_4$. Asymmetry is therefore a crucial property of the overlap measure and differs from other proposed measures, such as Cont and Schaanning (2018).

Returning to the derivation, the coefficient of determination serves as a useful starting point for constructing such an asymmetric measure. Similar to the two-bank situation above, we can calculate the R^2_i from a multiple regression of each $bank_i$ on all remaining banks,

$$bank_i = \sum_{j \neq i} bank_j\beta_j + u_i.$$

This coefficient R^2_i measures how well $bank_i$'s portfolio is *jointly* explained by the portfolios of all other banks. However, we are interested in the individual contributions of the banks on

[4] For example, if $bank_i = [1, 1, 1, 0, 0, 0]$ and $bank_j = [0, 0, 0, 1, 1, 1]$, the correlation is exactly -1. For a more elaborate example, consider the hypothetical system in the Appendix. The correlation between $bank_4$ and $bank_5$ would violate the non-negativity property as well, since $\rho_{4,5} = \text{corr}(bank_4, bank_5) < 0$.

the right-hand side. A decomposition of the R_i^2 into $N-1$ separate *partial*-$R_{i,j}^2$ would reflect the *relative importance* of $bank_j$ in explaining $bank_i$, compared to its peers. Denoting the decomposition function with d, we have $d(R_i^2) := [R_{i,1}^2, ..., R_{i,j}^2, ..., R_{i,N}^2]$. Note that we define a bank's overlap with itself as zero, $R_{i,i}^2 = 0$. These partial-R^2 capture the essence of our portfolio overlap measure. They are, by construction, non-negative; allow the overlap measure to be asymmetric; and depend on which banks and assets are considered in their calculation.[5] To compute the overlap relationships for the entire system, we repeat this exercise for all banks. Each repetition yields a row vector of partial-R^2. Stacking these results in the portfolio overlap matrix W, which will play a key role in the contagion modeling.

$$W := \begin{bmatrix} d(R_1^2) \\ \vdots \\ d(R_i^2) \\ \vdots \\ d(R_N^2) \end{bmatrix} = \begin{bmatrix} [\ 0 & \cdots & R_{1,j}^2 & \cdots & R_{1,N}^2] \\ & \vdots & & \vdots & \\ [R_{i,1}^2 & \cdots & 0 & \cdots & R_{i,N}^2] \\ & \vdots & & \vdots & \\ [R_{N,1}^2 & \cdots & R_{N,j}^2 & \cdots & 0\ ] \end{bmatrix} \tag{1}$$

3 Analytical framework

In this section, we construct a framework that embeds W into established credit spread models. After introducing the baseline regression model, we extend it with constant network effects and later on, introduce time-variation in these effects.

3.1 Baseline model

We start with a model similar to the structural regression of Collin-Dufresne et al. (2001).

$$\begin{aligned} \Delta CDS_{i,t} = {} & \gamma_i^1 R_t^{EU} + \gamma_i^2 \Delta slope_t^{EU} + \gamma_i^3 \Delta vola_t^{EU} \\ & + \delta_i^1 R_t^C + \delta_i^2 \Delta slope_t^C + \delta_i^3 \Delta yield_t^C \\ & + \theta_i^1 R_{i,t} + \theta_i^2 lev_{i,t} + const_i + e_{i,t}, \qquad \text{with} \quad e_{i,t} \sim N(0, \sigma_i^2). \end{aligned} \tag{2}$$

The explanatory variables are described in Table 2 in the data section and are grouped in three categories: European-wide, country-wide, and bank-specific. To simplify notation, we stack the N equations and collect all K regressors in one regressor matrix:

$$y_t = X_t \beta + e_t, \qquad \text{with} \quad e_t \sim N(0, \Sigma). \tag{3}$$

Note that β contains bank-specific regression coefficients as in Collin-Dufresne et al. (2001) and that the covariance matrix is heteroskedastic with $\Sigma = \text{diag}(\sigma_1^2, ..., \sigma_N^2)$. Furthermore, the

[5] While R^2 decomposition is not a trivial task, the statistical literature on relative importance and variable selection has proposed several methods for it. We refer the reader to the Appendix for the algorithm and accompanying technical discussion of our overlap measure.

empirical application also includes the lagged variables y_{t-1}, X_{t-1} as regressors.

3.2 Network effects model

As discussed in the introduction, we distinguish between two types of network effects, namely *structural network effects* and *residual network effects*. Correspondingly, we introduce the same portfolio overlap network W into the baseline model (2) in the different two ways.

Structural network effects refer to changes in one bank's credit risk that are due to changes in a neighboring bank's credit risk. To incorporate this effect, we extend the baseline model (2) by allowing $y_{i,t}$ to be influenced by other $y_{j,t}$, according to the similarities in ρW:

$$y_t = \rho W y_t + X_t\beta + e_t. \tag{4}$$

Here, $\rho \in [0, 1)$ is the *structural network intensity*. If $\rho = 0$, the structural network effects model (4) reverts back to the baseline (2). The overlap matrix W is calculated according to Algorithm 1, described in the Appendix. By repeatedly inserting (4) into itself, it becomes clear how information spillovers happen through W.

$$\begin{aligned} y_t &= \rho W y_t + X_t\beta + e_t \\ &= \rho W(\rho W y_t + X_t\beta + e_t) + X_t\beta + e_t \\ &= \rho W(\rho W(\rho W y_t + X_t\beta + e_t) + X_t\beta + e_t) + X_t\beta + e_t \\ &= \cdots = \lim_{m\to\infty} \sum_{n=1}^{m} [\rho W]^n (X_t\beta + e_t) \end{aligned} \tag{5}$$

The process in equation (5) converges to a fixed point if the largest eigenvalue of ρW is smaller than one in absolute value. Since W is row-stochastic by construction, its largest eigenvalue is exactly equal to one and, therefore, the invertibility condition reduces to $|\rho| < 1$. In this case, we can express the model in explicit form.

$$\begin{aligned} y_t &= (I_N - \rho W)^{-1} X_t\beta + (I_N - \rho W)^{-1} e_t \\ y_t &= Z X_t\beta + Z e_t \\ y_t &= Z X_t\beta + \epsilon_t \qquad \text{with} \quad \epsilon_t \sim N(0, Z\Sigma Z^\top) \end{aligned} \tag{6}$$

Here, $Z = (I_N - \rho W)^{-1}$ is the structural network component. Note that it affects both regressors and errors. We also define $\epsilon_t = Z e_t$ as *dirty* model errors, as their covariance matrix $Z\Sigma Z^\top$ is not diagonal. This differentiates them from clean model errors e_t.

Economic interpretation The last line in equations (5) contains the keystone of our model: In the limit, the endogenous structure vanishes and the dependent variable can be isolated from the independent variables. Economically, this model stipulates that the observed CDS

prices are the *consensus* prices of the market participants. This consensus finding process is driven by the information contagion about the underlying banks. The course of the spillover process is determined by the portfolio overlap network W, while its duration is controlled by the network intensity ρ. Thus, (4) stipulates that one bank's CDS price depends on the CDS prices of its peers. But if we follow this logic to the end, then the price in (6) ultimately depends on both the exogenous credit determinants of its peers and their idiosyncratic errors. The dependence on peers' risk determinants has two important implications. First, this framework establishes a new channel between one bank's credit risk and another bank's credit determinant. Secondly, even though the clean model errors e_t are independently distributed with diagonal covariance matrix Σ, the dirty model errors ϵ_t are 'tainted' from the contagion process and have a covariance structure $Z\Sigma Z^\top$. The resulting heteroskedasticity and cross-correlations between individual idiosyncratic shocks is determined by the overlap matrix W. To isolate both effects, we can also model the effects in the residuals separately.

Residual network effects While structural network effects introduce contagion into both regressors and residuals, the residual network effects model only does so for the latter. The mechanism is as described before and relies on the same overlap matrix W. To differentiate, we use λ to denote the residual network intensity.

$$y_t = X_t\beta + u_t \qquad \text{with} \quad u_t = \lambda W u_t + e_t \tag{7}$$

Under the condition that $|\lambda| < 1$ we can write the model into explicit form.

$$\begin{aligned} y_t &= X_t\beta + (I_N - \lambda W)^{-1} e_t \\ y_t &= X_t\beta + \Lambda e_t \\ y_t &= X_t\beta + \epsilon_t \qquad \text{with} \quad \epsilon_t \sim N(0, \Lambda\Sigma\Lambda^\top) \end{aligned} \tag{8}$$

Here, $\Lambda = (I_N - \rho W)^{-1}$ denotes the residual network component. Note that the structural network effects and residual network effects are identical if the data-generating process does not contain any exogenous determinants.

Lastly, we define a network effects (NE) model that contains both network effects.

$$y_t = \rho W y_t + X_t\beta + u_t \qquad \text{with} \quad u_t = \lambda W u_t + e_t \tag{9}$$

Under the same invertibility conditions we can reformulate (9) into the explicit form

$$\begin{aligned} y_t &= (I_N - \rho W)^{-1} X_t\beta + (I_N - \rho W)^{-1}(I_N - \lambda W)^{-1} e_t \\ y_t &= Z X_t\beta + Z\Lambda e_t \\ y_t &= Z X_t\beta + \epsilon_t \qquad \text{with} \quad \epsilon_t \sim N(0, Z\Lambda\Sigma\Lambda^\top Z^\top) \end{aligned} \tag{10}$$

Figure 2: Timeline overview of DNE model

This figure outlines the three frequencies in the DNE model. The overlap matrix W, which proxies the bank business model similarities, is calculated at the beginning of each quarter, the CDS spreads are daily, and the contagion process takes place within each day. The bar charts depict the geometric convergence behind the network effects from (5). The left panel ($t = 1$), describes how network effects (black) are added to the initial, exogenous value $X_1\beta$ until the total effects (white) converge to the observed CDS price y_1.

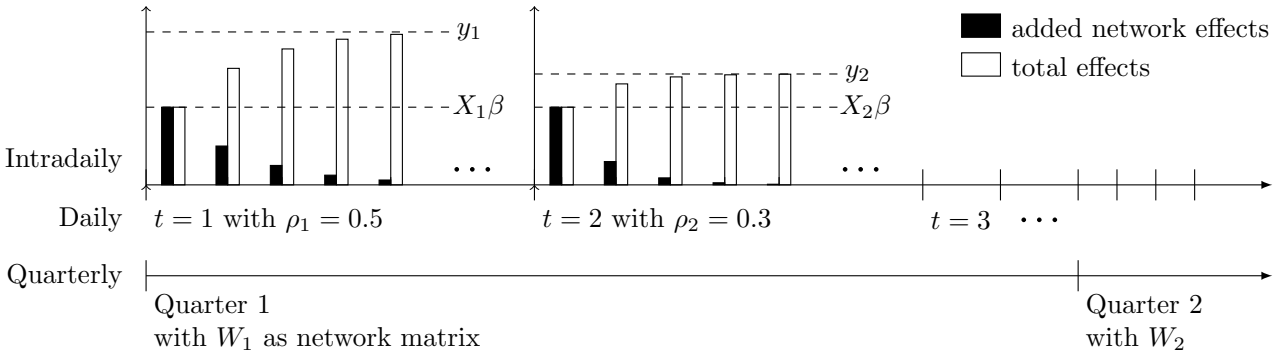

3.3 Dynamic network effects model

Since we suspect that the intensity of information contagion does not remain constant across time, we introduce time variation in the network effects $\rho_t W_t$ and $\lambda_t W_t$, respectively. We assume that the time dynamics are primarily driven by the intensity parameters ρ_t and λ_t. In fact, they vary on the same daily frequency as the credit spreads y_t, while W_t varies only on a quarterly frequency. See Figure 2 for an overview of the temporal structure in the model. This frequency is primarily dictated by the data availability. However, even if a daily frequency were available, we would still have used a lower frequency for two reasons: First, banks are not likely to change their profiles significantly over time. Roengpitya et al. (2014) point out that most of the 108 banks they investigate remain in the same classification. Commercial banks switched between retail to wholesale funding before and after the crisis, but this happened within a period of six years. In their subsequent study about model popularity and transitions, Roengpitya et al. (2017) use the bank-year as their time unit and find that in the period from 2006 to 2015, European banks switched business models on average 1.25 times. Thus, even though models are not static, they certainly do not shift from one day to the next. Second, if W_t were to change daily along with ρ_t and λ_t, we would face an endogeneity problem in the estimation. The data-generating process assumes that information contagion happens for given perceptions of the bank similarities.

However, if the underlying similarities can change as a result of information spillovers, then simultaneity will lead to biased estimates of the network effects. To model and estimate the dynamic intensity parameters ρ_t and λ_t we treat them as latent state variables within a state-space framework (Durbin and Koopman, 2012). For the network models to be invertible we need to ensure that ρ_t and $\lambda_t \in [0, 1)$. Hence, we do not model the time-dynamics directly but instead model two state variables α_t^1, α_t^2. These, in turn, drive the intensities $\rho_t = \Phi(\alpha_t^1)$ and $\lambda_t = \Phi(\alpha_t^2)$ through a logistic transformation function $\Phi : \mathbb{R} \to [0, 1)$. The final state-space model is described below.

DYNAMIC NETWORK EFFECTS (DNE) MODEL

Observation equation

$$y_t = Z_t X_t \beta + \epsilon_t \qquad \text{with} \quad \epsilon_t \sim N(0, Z_t \Lambda_t \Sigma \Lambda_t^\top Z_t^\top),$$

with $Z_t = (I - \rho_t W_t)^{-1}$ and $\Lambda_t = (I - \lambda_t W_t)^{-1}$ and covariance matrix $\Sigma = \sigma^2 I_N$.

State equations

$$\alpha_t^1 = c_1 + T_1 \alpha_{t-1}^1 + \eta_t^1 \qquad \text{with} \quad \eta_t^1 \sim N(0, \sigma_1^2),$$
$$\alpha_t^2 = c_2 + T_2 \alpha_{t-1}^2 + \eta_t^2 \qquad \text{with} \quad \eta_t^2 \sim N(0, \sigma_2^2),$$

with $\rho_t = \Phi(\alpha_t^1)$ and $\lambda_t = \Phi(\alpha_t^2)$ where $\Phi : \mathbb{R} \to [0, 1)$ is a logistic transformation.

Estimation methodology While the Kalman filter can estimate the linear baseline model, with regression coefficients as constant state variables, the DNE model is highly nonlinear due to the contagious process in the observation equation. Furthermore, the model includes heteroskedasticty and stochastic volatility, since the time-varying network effects also affect the residuals. These properties make the estimation a challenging task and linear estimators like the Kalman filter are not applicable. Approximating nonlinear filters, such as the extended or unscented Kalman filter, do not perform satisfactorily either, mostly due to the stochastic volatility5. Therefore, we estimate our nonlinear state-space model with a smooth marginalized particle filter, based on the smooth particle filter (Malik and Pitt, 2011; Doucet et al., 2001) and the marginalized particle filter (Schön et al., 2006). This simulation-based filter is able to cope with all of the DNE model's properties and has the best performance of all filters we have examined. We discuss details of this estimator's performance and its finite sample properties using an extensive simulation study in the companion paper Wang et al. (2018).

4 Data

We study contagion among the 22 largest banks or banking groups with headquarters in the Eurozone for the period from January 01, 2014, to June 30, 2016. These banks are located in seven countries: Austria, Belgium, France, Germany, Italy, Netherlands, and Spain. To maintain confidentiality, we present results for Austria and Germany as AT, DE and Belgium and Netherlands as BE, NL. We use the daily 5-year senior, full-restructuring CDS spreads for the dependent variable, as they are the most commonly traded credit derivative contract (Augustin et al., 2014).[6] The set of structural regressors can be broken down into three groups: 1) Europe-wide, 2) country-wide, and 3) bank-specific. Measures included are,

[6]See Ericsson et al. (2009) for the advantages of using CDS spreads over calculated credit spreads.

amongst others, the slope of the yield curve, stock market performance and leverage (see Table 2). We interpolate the quarterly available data to match the daily frequency of other regressors. To calculate the portfolio overlap network according to Algorithm 1, we use the reported holdings data from the Securities Holdings Statistics (SHS). This data is reported on a quarterly basis and covers each of the 22 banks' holdings in about 250,000 unique securities, identified by their International Securities Identification Number (ISIN). For confidentiality reasons, the calculated networks cannot be shown here. The networks experience only slight variations between quarters and have many within-country but few between-country overlaps.

5 Empirical analysis

We begin by estimating the benchmark model and replicating the two established stylized facts of the credit spread puzzle: First, the low explanatory power of the structural regressors in terms of R^2; and, second, the presence of a common factors in the regression residuals. Next, we estimate a model with constant network effects (NE) model to see if this improves model performance. Finally, we analyse a Dynamic Network Effects (DNE) model which can show us how much we gain through time-variation in the network effects.

5.1 Baseline model

Table 3 presents the regression results of the linear baseline model. Due to the confidentiality reasons, we present the results as group averages. We also present the anonymized regression coefficients in density plots (Figure 5a and 8a, upper halves) and the associated p-values in histograms (Figure 5b and 8b, upper halves).

For Europe-wide regressors, we find that the sign and magnitude of the group averages are mostly homogeneous. In line with previous research, higher equity returns and proxy for the yield curve slope are associated with lower credit spreads while the opposite holds for volatility indicators.[7] Similarly, the bank-specific regressors have the same signs across each group. The constant is insignificant for all banks while equity returns are significantly negative for half of the banks, most notably for Spain and Italy. For country-specific regressors, the group averages are more heterogeneous. Once again, we rediscover a North-South division where Italian and Spanish bank spreads respond similarly to their countries' 10-year bond yields and yield curve slopes, while the Austria, Belgium, France, Germany and Netherlands point to the opposite direction. Leverage is insignificant, most clearly seen in the p-value histograms (Figure 5b and 8b). This is likely due to its low, quarterly frequency in contrast to the high, daily frequency of the spread changes.

[7]Note that the parentheses contain average p-values for each group and hence cannot used directly for the rejection of the null hypothesis.

Table 1: Bank groups and data availability

Bank	Abbreviation	Country	CDS data	Stock price
KBC Bank NV	kbc	BE	01 Jan 2014	01 Jan 2014
ABN AMRO Bank NV	abn	NL	01 Jan 2014	20 Nov 2016
ING Group	ing	NL	01 Jan 2014	01 Jan 2014
Rabobank	rabo	NL	01 Jan 2014	Not listed
BNP Paribas	bnpp	FR	01 Jan 2014	01 Jan 2014
Groupe BPCE	bpce	FR	02 Jul 2015	Not available
Crédit Agricole	cagricole	FR	01 Jan 2014	01 Jan 2014
Crédit Mutuel	cmutuel	FR	01 Jan 2014	Not available
Société Generale	socgen	FR	01 Jan 2014	01 Jan 2014
Erste Bank Group AG	erste	AT	01 Jan 2014	01 Jan 2014
Bayerische Landesbank	bayernlb	DE	01 Jan 2014	Not listed
Commerzbank AG	commerz	DE	01 Jan 2014	01 Jan 2014
Deutsche Bank AG	deutsche	DE	01 Jan 2014	01 Jan 2014
Deutsche Pfandbriefbank AG	dpbb	DE	01 Jan 2014	01 Jan 2014
DZ Bank AG	dzbank	DE	01 Jan 2014	Not listed
Landesbank Baden-Württemberg	lbbw	DE	01 Jan 2014	Not listed
Norddeutsche Landesbank	nordlb	DE	09 May 2014	Not listed
Banca Monte dei Paschi di Siena SpA	bmps	IT	01 Jan 2014	01 Jan 2014
Intesa Sanpaolo SpA	intesa	IT	01 Jan 2014	01 Jan 2014
UniCredit SpA	unicredit	IT	01 Jan 2014	01 Jan 2014
Banco Bilbao Vizcaya Argentaria SA	bbva	ES	01 Jan 2014	01 Jan 2014
BFA Tenedora de Acciones SAU	bfa	ES	01 Jan 2014	01 Jan 2014
CaixaBank SA	caixa	ES	01 Jan 2014	01 Jan 2014
Santander Group	santander	ES	01 Jan 2014	01 Jan 2014

Table 2: Data of independent variables

Variable	Description	Freq.	Source
EUROPE-WIDE			
R_t^{EU}	Log-returns of EuroStoxx50	D	Bloomberg
$slope_t^{EU}$	Difference between 10-year Euro swap rate and 3-month EURIBOR	D	Bloomberg
$vola_t^{EU}$	EuroStoxx50 Volatility (VSTOXX)	D	Bloomberg
COUNTRY-WIDE			
R_t^C	Log-returns of ATX, BEL20, DAX, IBEX35, CAC40, FTSE MIB, AEX	D	Bloomberg
$yield_t^C$	10-year sovereign bond yield	D	Bloomberg
$slope_t^C$	Difference between 10-year and 2-year sovereign bond yields	D	Bloomberg
BANK-SPECIFIC			
$R_{i,t}$	Log-differences of stock prices, if available (see Table 1)	D	Bloomberg
$lev_{i,t}$	Leverage ratio $lev_{i,t} = Tier\ 1\ captial_{i,t} / Total\ exposure\ measure_{i,t}$	Q	Bloomberg
$const_i$	Constant term	–	–

Furthermore, we confirm the two stylized facts of the credit spread puzzle: Higher than what Collin-Dufresne et al. (2001) found for U.S. corporate bonds, the group R^2 values range from 22.32% (Austria, Germany) to 43.16% (Italy) with an total average of 28.39%. To determine whether this indicates a good model performance we turn our attention to the residuals, which we assume to be orthogonal. In Figure 3, we find the reverse in a systematic common factor across all banks. This factor alone explains 40.41% of the residual variance, while the first four components together make up 56.78%. Interestingly, the second component seems to capture country-specific effects, even though the regression model already includes country-specific regressors. Upon closer inspection, the component draws a line between Northern and Southern Eurozone members. Thus, the residuals curiously still reflect the North-South divide, even though it was already a feature of the country-specific regressors. Fontana and Scheicher (2016) find a similar division for European sovereign CDS spreads.

Figure 3: Principal components analysis of baseline residuals

This graph presents the coefficients of the four largest principal components of the baseline model residuals. We see that the first component is a systematic factor that affects all banks. Furthermore, the second component is a North-South factor that assigns positive values to Austria, Belgium, Germany, France, Netherlands and negative values to Italy, Spain.

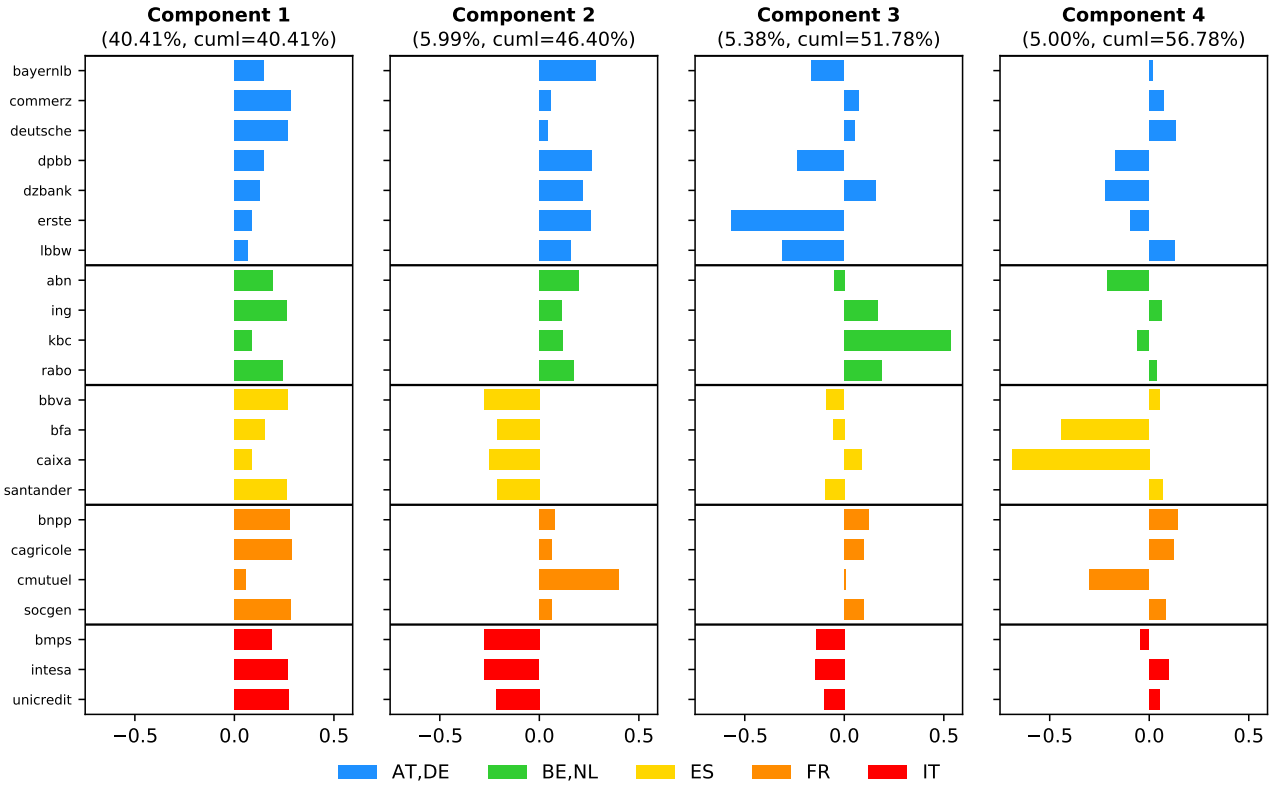

Table 3: Regression results of baseline model

This table presents the regression coefficients of each country group (see Table 1). For confidentiality reasons, we present group averages. Note that the parentheses contain average p-values and therefore do not lend themselves for hypothesis testing. The bottom rows present the average R^2 coefficient of each group.

		Average	Country group				
Scope	Variable	All banks	BE,NL	ES	FR	AT,DE	IT
Europe	$eurostoxx50$	-0.9941	-0.7913	-0.6494	-1.7427	-0.9150	-0.9102
		(0.2142)	(0.1788)	(0.3120)	(0.0093)	(0.3414)	(0.1076)
	$slope^{EU}$	-0.1433	0.0839	-0.3774	-0.0396	-0.0705	-0.4424
		(0.3728)	(0.3784)	(0.2595)	(0.4953)	(0.4416)	(0.1928)
	$vstoxx$	0.1274	-0.1201	0.2596	0.1098	0.1208	0.3200
		(0.4765)	(0.2050)	(0.4552)	(0.5802)	(0.6646)	(0.2900)
	$L.eurostoxx50$	-0.3548	-0.0904	-0.2708	-0.6272	-0.5620	0.0272
		(0.3983)	(0.3196)	(0.6357)	(0.2077)	(0.3419)	(0.5722)
	$L.slope^{EU}$	-0.0354	-0.1858	-0.0470	0.1676	-0.0297	-0.1037
		(0.5642)	(0.5037)	(0.7718)	(0.4604)	(0.4956)	(0.6663)
	$L.vstoxx$	0.2378	0.1894	0.3182	0.1152	0.2844	0.2499
		(0.3856)	(0.3780)	(0.3312)	(0.5488)	(0.3490)	(0.3358)
Country	$bond10y^C$	0.0081	-0.0714	0.4490	-0.6194	-0.2207	0.8971
		(0.2386)	(0.1831)	(0.1645)	(0.2035)	(0.3773)	(0.1342)
	$eqidx^C$	-0.1525	-0.4413	-0.4494	0.6270	-0.2518	-0.1792
		(0.3531)	(0.2924)	(0.5201)	(0.1266)	(0.3277)	(0.5728)
	$slope^C$	0.2081	0.0967	-0.0333	0.5915	0.3620	-0.1917
		(0.1727)	(0.2408)	(0.0686)	(0.0920)	(0.2764)	(0.0868)
	$L.bond10y^C$	-0.0177	0.3144	-0.3465	-0.2802	0.1354	-0.0296
		(0.4311)	(0.5123)	(0.4270)	(0.4634)	(0.3497)	(0.4752)
	$L.eqidx^C$	0.2054	-0.0580	0.0738	0.3724	0.4843	-0.1415
		(0.3549)	(0.3848)	(0.5307)	(0.1539)	(0.2897)	(0.5006)
	$L.slope^C$	0.0400	-0.2118	0.3306	0.2564	-0.1460	0.1335
		(0.4629)	(0.5322)	(0.4247)	(0.3078)	(0.4915)	(0.5615)
Bank	$const$	0.0698	0.0522	0.0837	0.0738	0.0427	0.1329
		(0.6016)	(0.7364)	(0.5759)	(0.4346)	(0.7511)	(0.3298)
	eq	-0.3464	-0.1974	-0.5461	-0.2850	-0.1672	-0.7793
		(0.3267)	(0.4380)	(0.0206)	(0.2285)	(0.6342)	(0.0000)
	lev	-0.0048	-0.0133	0.0271	0.0343	-0.0489	0.0147
		(0.5220)	(0.3922)	(0.4670)	(0.7427)	(0.4481)	(0.6463)
	$L.cds$	-0.2820	-0.1956	-0.3766	-0.0672	-0.5371	0.0380
		(0.2660)	(0.3877)	(0.2765)	(0.2833)	(0.1800)	(0.2673)
	$L.eq$	-0.1281	-0.0605	-0.0599	-0.1782	-0.2056	-0.0614
		(0.4457)	(0.6376)	(0.4818)	(0.2439)	(0.5496)	(0.1683)
R^2	Baseline	0.2839	0.2582	0.3072	0.2816	0.2232	0.4316
	Observations	22	4	4	4	7	3

5.2 Network effects model

In this section, we present the results from the NE model and compare them with the baseline model. In contrast to the baseline model, we also obtain estimates for the latent network intensity parameters, $\hat{\rho} = 0.244$ and $\hat{\lambda} = 0.351$. These correspond to a structural multiplier effect of 1.324 and residual multiplier effect of 1.542.

Our first main result focuses on how the regression coefficients adjust in response to the network effects. The violin plots in Figure 5a visualize this difference for each coefficient and Figure 5b displays their change in statistical significance.[8]
After including network effects, the coefficient averages generally decrease in absolute value. The density distributions tend to become less dispersed and move closer to zero. Compared to the baseline model, bank-specific regressors become more significant as a higher fraction of them falls below the 5% significance threshold, such as leverage or lagged credit spreads. The volatility indicator also becomes more significant. Across all scopes, equity-related regressors lose economic significance. At the same time, they also become statistically less significant, with the exception of lagged country-level equity index returns. Thus, neglecting the network effects potentially overstates the importance of structural regressors.

The better fit is also reflected by the strictly higher share of explained variances.[9] The R^2_{dirty} based on prediction errors ranges from 22.79% (AT, DE) to 32.45% (IT) with a total average of 28.86%, which is only slightly higher than in the baseline model. We do not expect this improvement to be large, because the prediction errors, or dirty model residuals, still contain the contagion effects. After filtering out the contagion component, the R^2_{clean} based on clean residuals ranges from 33.11% (BE, NL) to 68.14% (IT) with an average of 42.86%, which is by 13.0% higher than in the baseline model.

Figure 4 depicts our second main result: After accounting for network effects, the largest component in the clean residuals only accounts for 19.94% of residual variance, less than half of its baseline counterpart. Furthermore, all four components account jointly for 41.12%, compared to 56.78% in the baseline. Most importantly, the first component loses its systematic nature. Its loadings are not strictly positive for all banks anymore, and some of them are very close to zero. Moreover, the second, North-South component loses its dividing character as its

[8] More detailed results are reported in Table 4, Appendix.

[9] The R^2 depends on how we compute sum of squared residuals. In the baseline model, we compute the R^2 using the sum of squared residuals, which are based on the prediction errors, $\hat{e}_t = y_t - \hat{y}_t$. In the NE model, however, prediction errors contain network effects (see equation (10)). We refer to them as 'dirty' model residuals, $\hat{\epsilon}_t$. Filtering out these effects yields 'clean' model residuals, $\hat{e}_t$.

dirty model residuals (prediction errors)	$\hat{\epsilon}_t = y_t - \hat{y}_t = \hat{Z}_t \hat{\Lambda}_t \hat{e}_t$
clean model residuals	$\hat{e}_t = \hat{\Lambda}_t^{-1} \hat{Z}_t^{-1} \hat{\epsilon}_t$

The two types of residuals lead to two corresponding R^2_{dirty} and R^2_{clean}.

values become more erratic with no clear pattern. This means that the overlap network both explains most of the unobserved, systematic residual component and accounts for country-specific effects that eluded the regressors.

We examine further residual diagnostics in Figure 11, Appendix. The left panel of Figure 12a shows how the average correlation of a bank's residuals with all other banks drops from 0.353 to 0.099 while also becoming less dispersed. On the right panel of Figure 12a we see a more pronounced effect for the squared residuals, dropping from 0.187 to 0.103. In the center, Figure 12b, we plot the p-values of a Ljung-Box test for autocorrelation across different lag horizons. The results show that the residuals become significantly more autocorrelated after including network effects. We examine the autocorrelation structure and find that the autoregressive coefficients become (more) negative for all banks. At the bottom, Figure 12c displays the p-values of an ARCH-LM test for conditional heteroskedasticity. In contrast to the increasing serial autocorrelation, we find ambiguous effects of including the network. While we find less statistical evidence for residual clustering for some banks, it increases for others while some remain largely unchanged. This suite of tests leads us to conclude that including network effects mostly affects the cross-sectional characteristics, as seen in the drop in average (sqaured) residual correlation.

Figure 4: Principal components analysis of NE residuals

This graph presents the coefficients of the four largest principal components of the NE model residuals. We see that the first component loses its systematic nature and explains half of the residual variance (19.94%), compared to its baseline counterpart (40.41%). Furthermore, the second component loses its North-South factor structure. The banks are anonymized and their position randomized within each group.

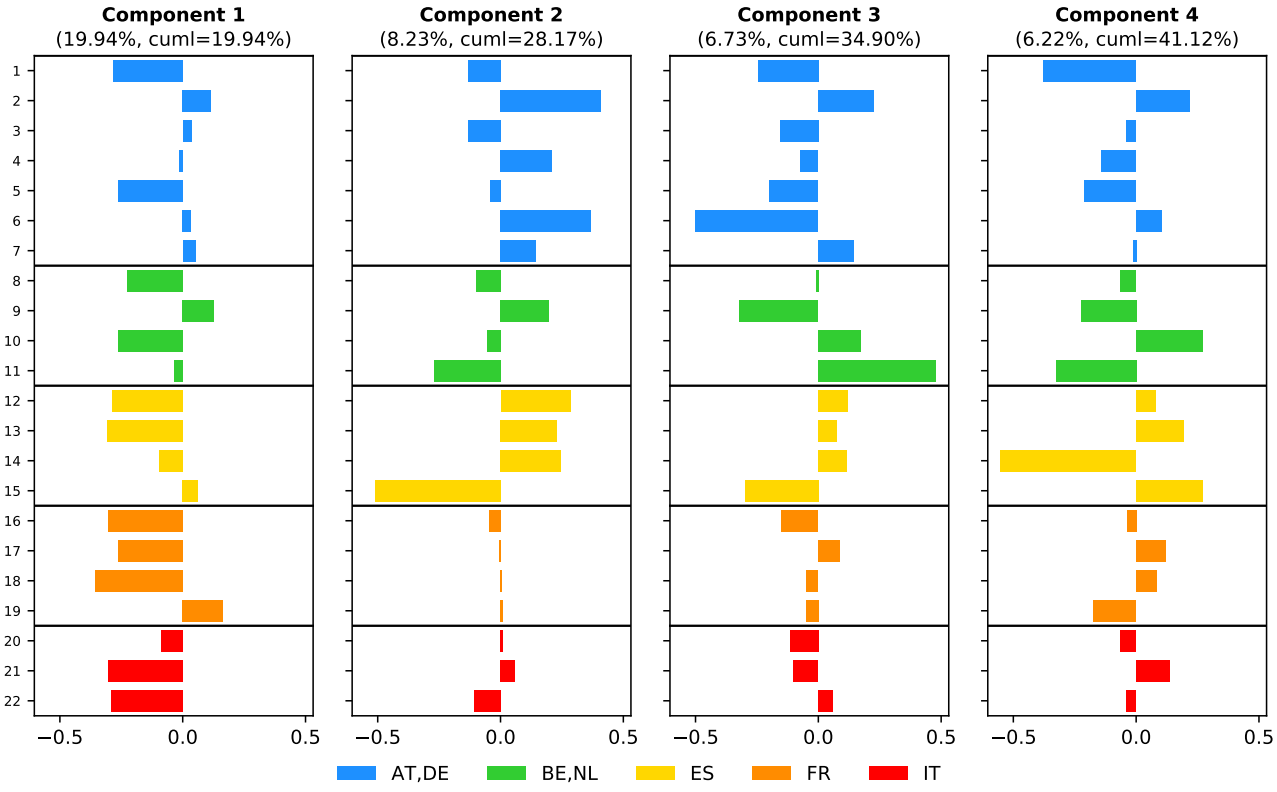

Figure 5: Regression results of baseline vs. NE models

The top, gray (bottom, white) halves of each plot depict the baseline (NE) model results. **(a)** presents the estimated coefficients as violin plots, where each thin black line marks the anonymized coefficient value of one bank. The triangles locate the average coefficient. **(b)** presents histograms of the corresponding p-values. The red line demarcates the 5% significance level. The triangles locate the average p-value.

(a) Violin plots of regression coefficients

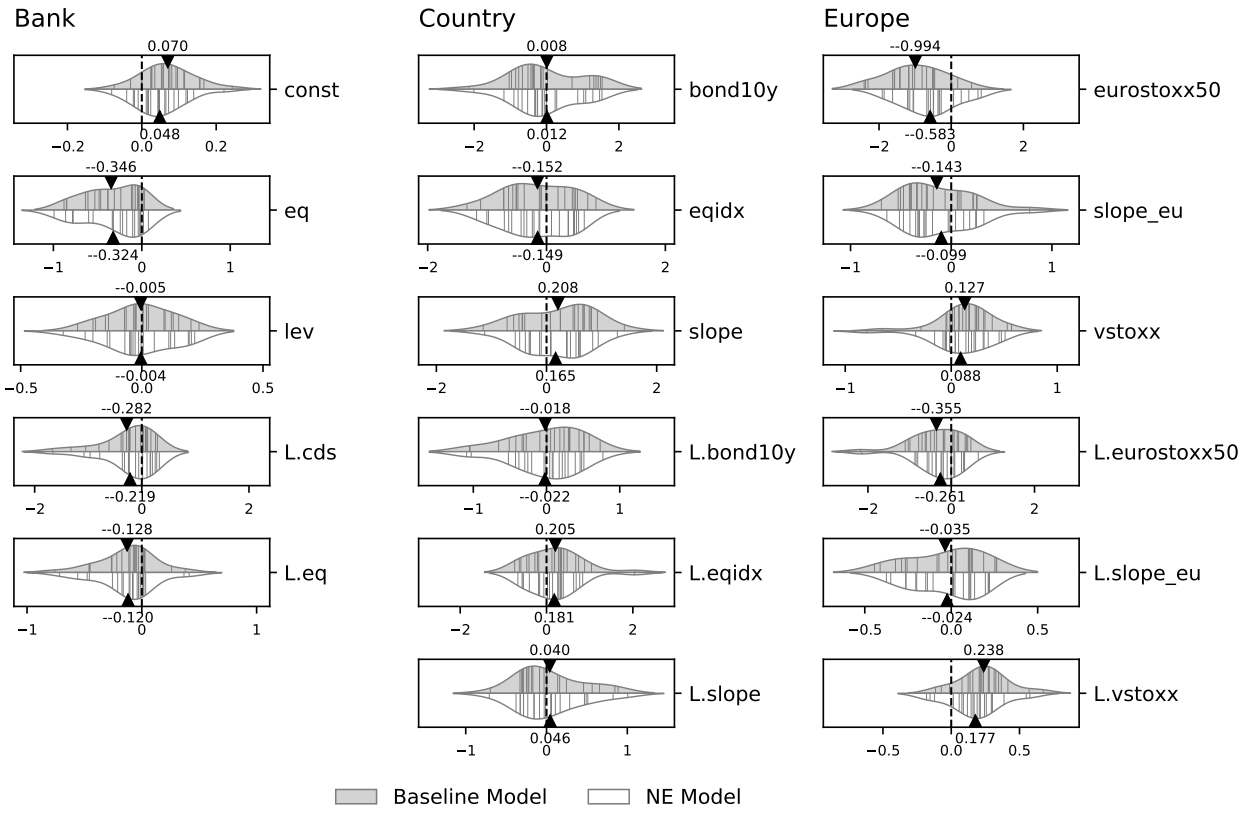

(b) p-values of regression coefficients

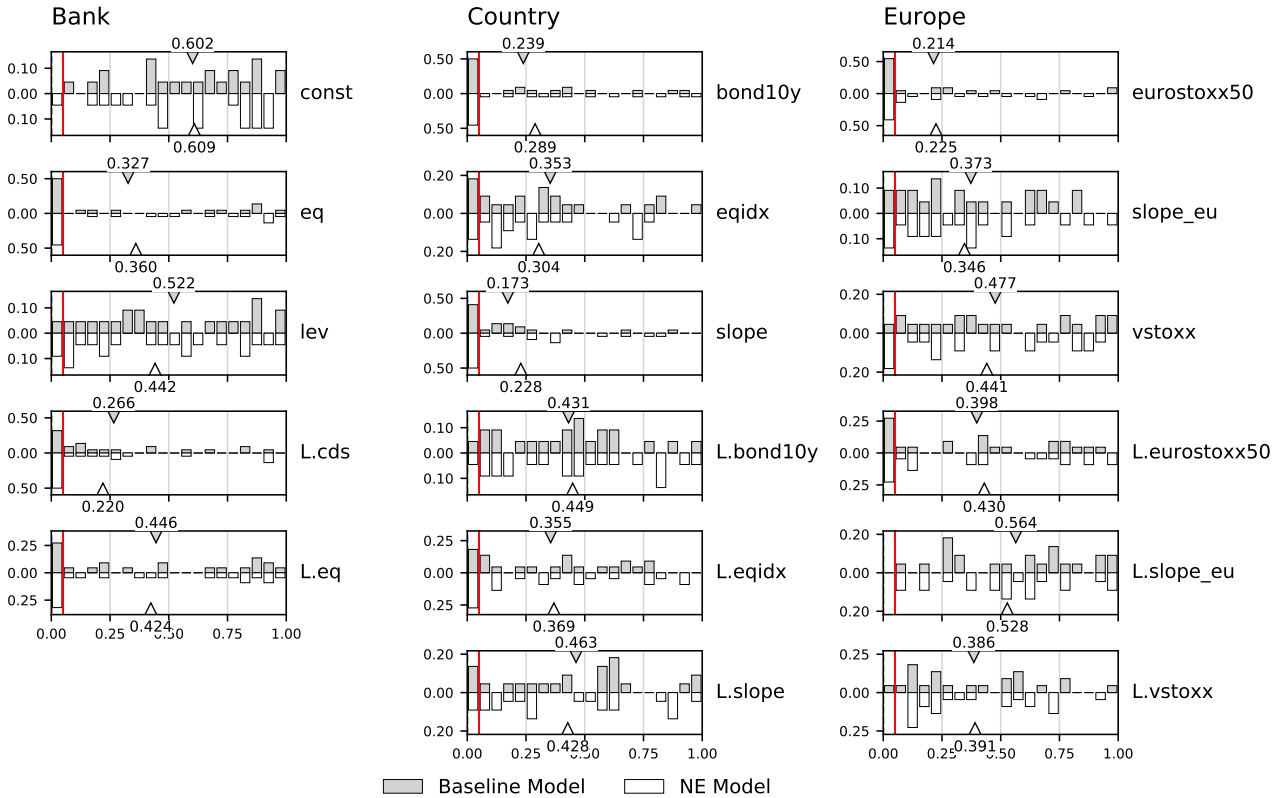

5.3 Dynamic network effects model

Arguably, if network effects exist, they are unlikely to remain constant over time. Figure 6 shows the estimated intensity parameters for both structural and residual network effects. The averages of both parameters ($\hat{\mathbb{E}}[\hat{\rho}_t] = 0.181$ and $\hat{\mathbb{E}}[\hat{\lambda}_t] = 0.404$) are close to their constant counterparts ($\hat{\rho} = 0.244$ and $\hat{\lambda} = 0.351$). These correspond to a structural multiplier effect of 1.221 and residual multiplier effect of 1.676. Their stationary nature also indicates that the added time-variation does not drastically alter the model results in relation to the constant case. Nonetheless, the plots reveal that the residual correlations according to the overlap matrix can vary significantly over time. The structural network effects in contrast amplify the structural component in a constant and moderate fashion. In the remainder of this section, we discuss the implications of the dynamic nature of the network effects.

As with the constant network effect model, we present the estimated coefficients in a violin plot (Figure 8a) and histograms for p-values (Figure 8b).[10] The results reproduce most of the findings of the constant network effects model. The coefficients move closer to zero and become less dispersed. However, the notable exception is the volatility index. Instead of decreasing in importance under constant network effects, it in fact becomes more significant in both economic and statistical senses. Table 5 reveals that this is primarily driven by the Southern banks.

The coefficients of determination also paint a similar picture as the constant case. The R^2_{dirty} ranges from 22.79% (AT, DE) with an average of 28.86%, which is 14.47% higher than in the baseline model. The R^2_{clean} ranges from 33.11% (BE, NL) with an average of 42.86%, which is almost 13.0% higher than in the baseline model. Thus, allowing the network effects to follow a stochastic process generally increases explanatory power. But this extension can also entail decreases, as in the case of the R^2_{clean} of Belgium and Netherlands.

This residual component analysis leads to only minor improvements as well (Figure 7). After accounting for dynamic network effects, the largest residual component accounts for 18.25% of residual variance, compared to 19.94% in the constant case. Furthermore, all four components account for 40.34% jointly, compared to 41.12% in the baseline. As before, the first and second components lose their distinct systemic and country structures. This leads us to conclude that dynamic network effects do improve model performance, but only marginally.

Table 11, Appendix presents further residual diagnostics. The DNE model lowers average (squared) residual correlations (Figure 12a) further than the NE model, but the improvements are almost indistinguishable from the constant specification. The same holds for the tests for serial autocorrelation (Figure 12b) and conditional heteroskedasticity (Figure 12c).

[10] Further results are shown in Table 5, Appendix.

Figure 6: Estimated network intensities ρ_t and λ_t

Estimated intensity parameters of the DNE model using a smooth marginalized particle filter: Structural network effects ρ_t (top, red) and residual network effects λ_t (bottom, blue). The 90% (50%) asymmetric confidence interval is demarcated with the light (dark) areas.

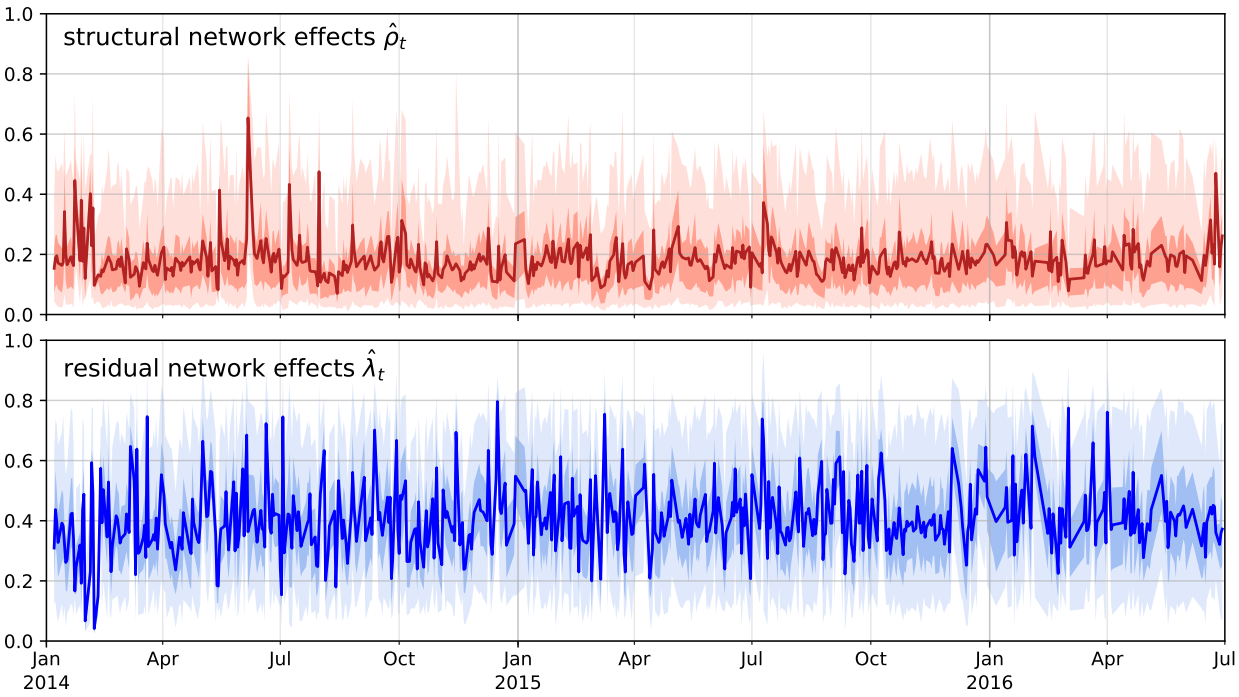

Figure 7: Principal components analysis of DNE residuals

This graph presents the coefficients of the four largest principal components of the DNE model residuals. We see that the first component loses its systematic nature and explains half of the residual variance (18.25%), compared to its NE counterpart (19.94%) or baseline counterpart (40.41%). Furthermore, the second component loses its North-South factor structure. The DNE model does outperform the NE model, but only slightly. The banks are anonymized and their position randomized within each group.

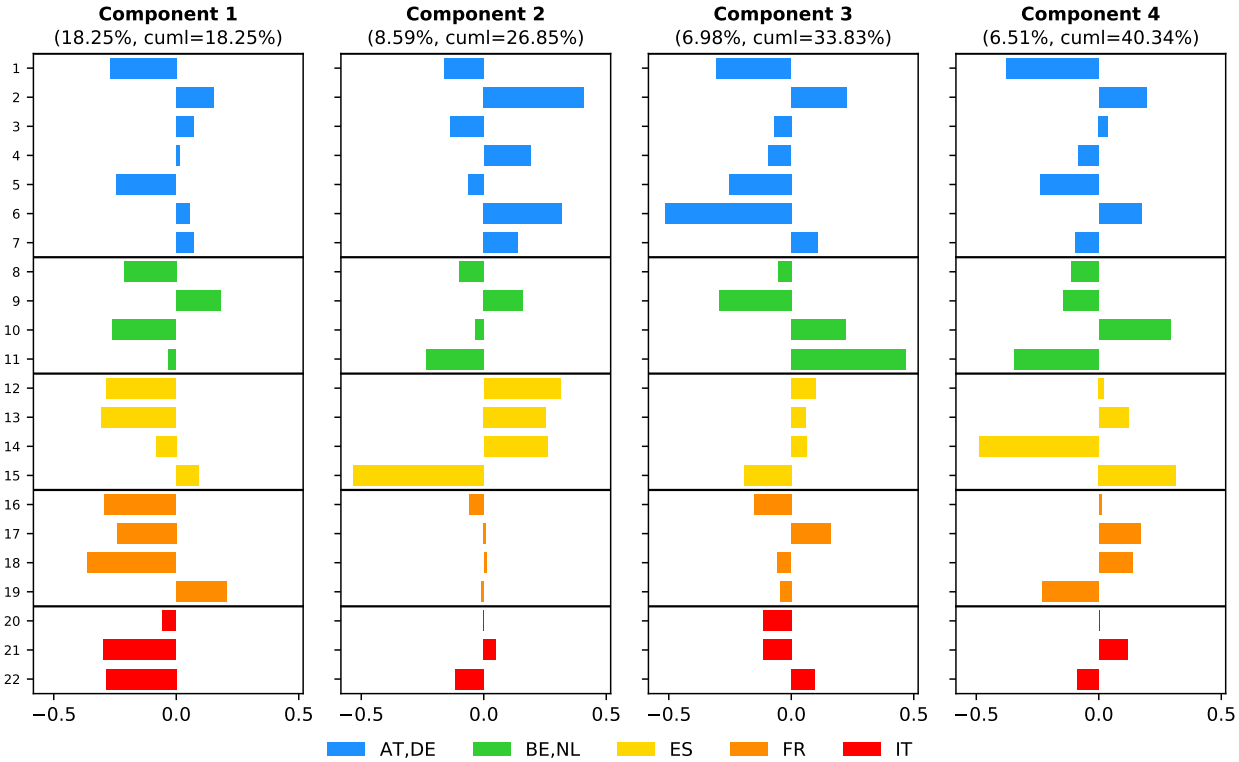

Figure 8: Regression results of baseline vs. DNE models

The top, gray (bottom, white) halves of each plot depict the baseline (DNE) model results. **(a)** presents the estimated coefficients as violin plots, where each thin black line marks the anonymized coefficient value of one bank. The triangles locate the average coefficient. **(b)** presents histograms of the corresponding p-values. The red line demarcates the 5% significance level. The triangles locate the average p-value.

(a) Violin plots of regression coefficients

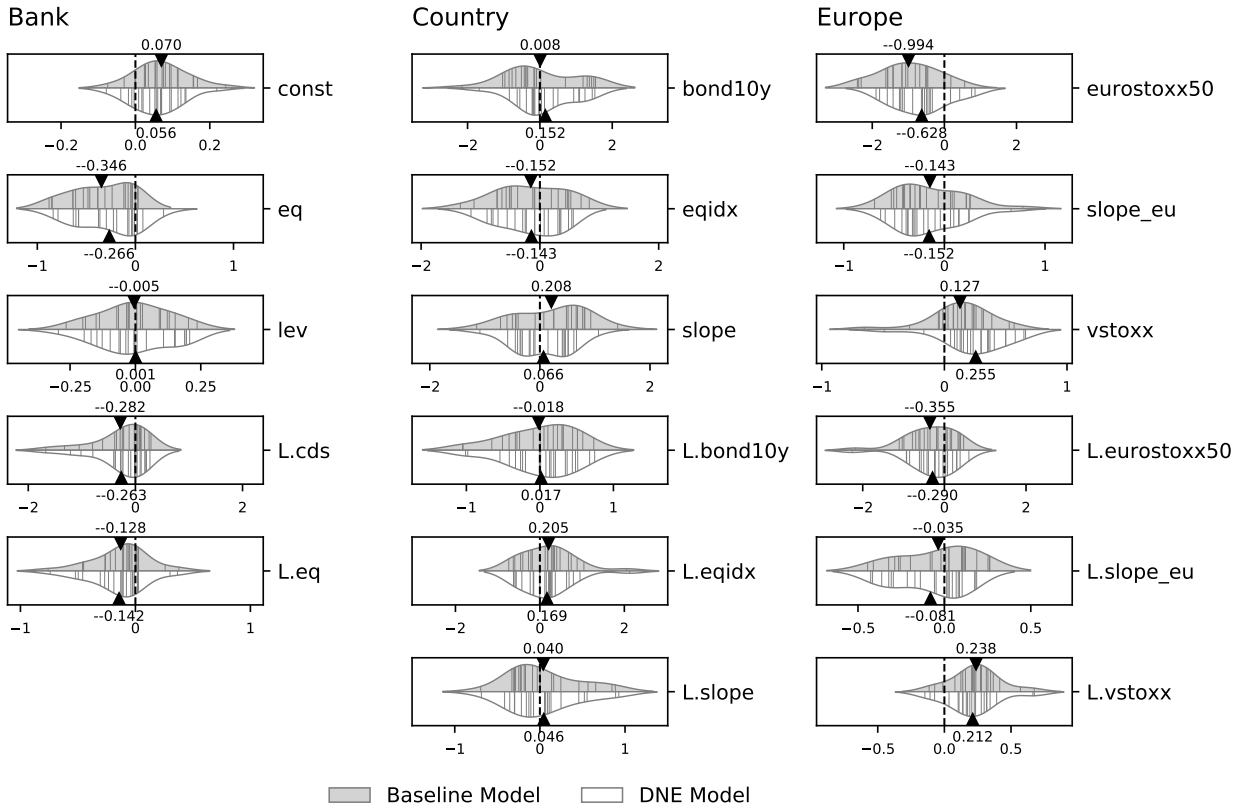

(b) p-values of regression coefficients

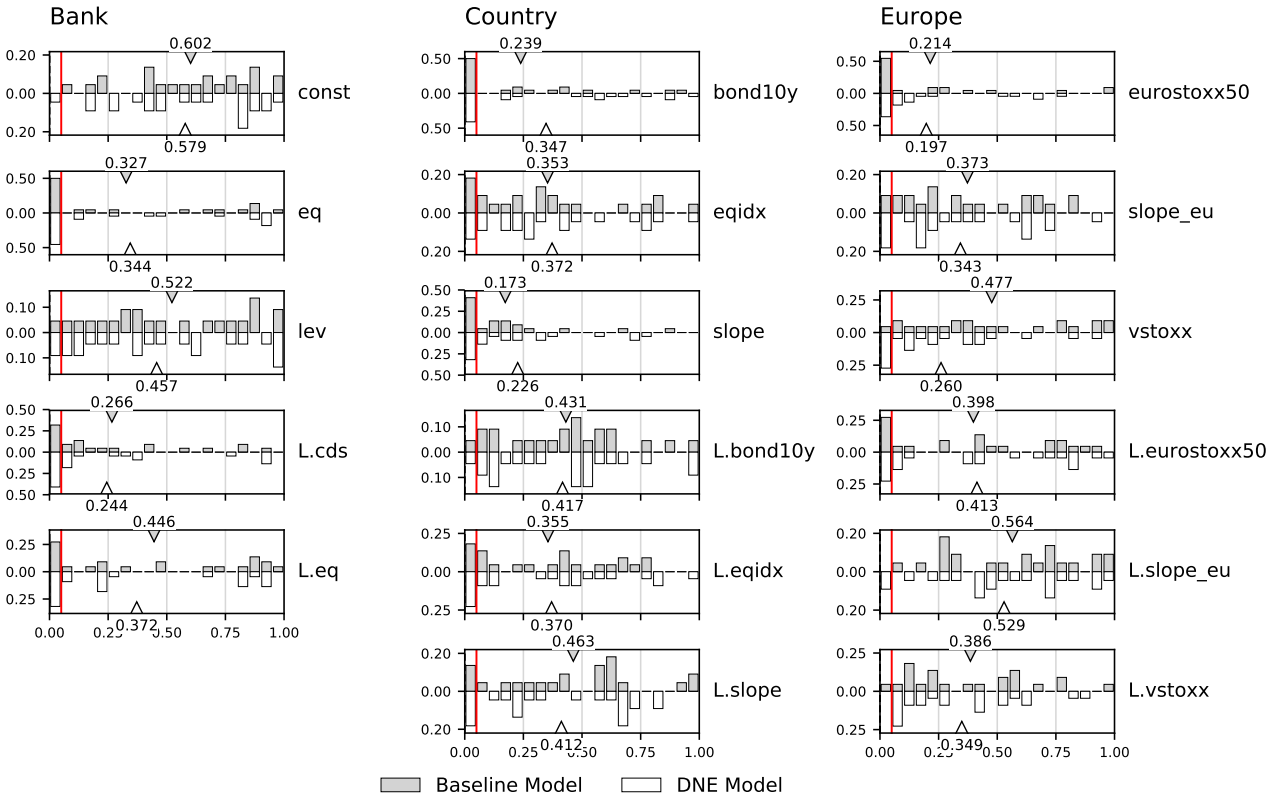

6 Conclusion

In this paper, we investigate whether incorporating business model similarities into the modeling of the credit spreads of the 22 largest banks in the Eurozone improves risk capture. Earlier models explain the credit spread based on structural regressors only, such as equity returns, market volatilities, and spot rates. These models suffer from low explanatory power and fail to capture a systemic common factor. We attribute their poor empirical performance – the *credit spread puzzle* – to the omission of contagion effects in the models. Such contagion could be driven by business model similarities, either real or perceived by the market. However, including such effects into linear regressions is challenging because contagion mechanisms are self-reinforcing and nonlinear. To address this limitation, we augment the existing models with a portfolio overlap network, positing that common asset exposures of banks are a reasonable measure of business model similarity. We construct the network by applying an R^2-decomposition method on the banks' complete holdings data. This leads to two extensions, the Network Effects (NE) model and Dynamic Network Effects (DNE) model. Both incorporate the overlap network and measure how important it is with intensity parameters. The difference is that the DNE model has time-varying intensities. If the network represents the vehicle that credit risk uses to spread from bank to bank, then the intensity represents the fuel that determines how far the vehicle can go. We obtain several surprising results with this modeling approach.

First, while the traditional model yields an R^2 for the European banks of 28.39% on average, the NE model leads to a higher R^2 for each bank, averaging 28.86%. After removing contagion effects in the residuals, the resulting average 'clean' R^2 goes up to 42.86%, an increase of 14.47% compared to the baseline model. We attribute the increased explanatory power to the NE's *structural network effects*. These effects include other banks as endogenous regressors, which ultimately still depend on the structural variables through the network. In addition, we find that the structural regressors of the NE become less important compared to the baseline. The DNE model, which has time-varying network effects, improves these findings even further, albeit only slightly. The average R^2_{clean} amounts to 43.02%. Surprisingly, while the regression coefficients generally become less relevant as in the NE model, the volatility index increases in importance under the DNE model. Thus, neglecting network effects, whether constant or dynamic, likely overstates the importance of most structural regressors. It is interesting to note that, although banks are presumably unaware of how much portfolio overlap they have with other banks, CDS premia nonetheless seem to correctly price this contagion risk. It should therefore be in the interest of regulators to monitor this risk channel.

Second, the residuals of traditional models contain uncaptured common factors. A principal component analysis reveals that the first component is a systematic factor that affects all banks, responsible for 40.41% of the remaining variance. The second component contains

country-specific blocks, which is surprising since the structural regressors already contain country-specific determinants. Upon closer inspection, this component differentiates between Northern countries (AT, BE, FR, DE, NL) and Southern countries (ES, IT). The NE and DNE models are constructed to capture these *residual network effects*. A subsequent residual component analysis confirms that the first component loses its systematic nature and only explains 19.94% (NE) and 18.25% (DNE) of the remaining variance, and the North-South factor component also loses its country-block structure. The largest four components jointly explain 41.12% (NE) and 40.34% (DNE) compared to 56.78% in the baseline. These findings imply that the portfolio overlap network helps us shed light on an aspect of credit risk that has eluded the structural regressors.

Lastly, the DNE allows us to measure the importance of the network effects over time. The structural network intensity oscillates around a constant mean of about $\hat{\mathbb{E}}[\hat{\rho}_t] = 0.181$ (corresponding to a multiplier of 1.221). At the same time, the residual network intensity revolves around $\hat{\mathbb{E}}[\hat{\lambda}_t] = 0.404$ (multiplier of 1.676). This intensity reaches 0.65 (multiplier of 2.85) during the market stress period of early 2016. The time-varying nature tells us that network effects respond to or predict periods of financial distress. The intensities also help us understand the contagion mechanism in details, for instance, by tracking how shocks to individual banks or Europe-wide variables find their way through the system during calm or volatile times.

In conclusion, we find that the portfolio overlap network and the NE/DNE frameworks are useful tools for understanding financial contagion and the credit spread puzzle, as well as their intricate relationship. The DNE model performs better than the NE model in every regard, as it allows for network effects to vary over time. But the improvements are slight, indicating that accounting for constant network effects is already sufficient to realize almost all of the benefits. Furthermore, it is likely that variables of market illiquidity will have explanatory power for the credit spreads as well. Doubtlessly, other contagion channels, such the interbank lending channel, play crucial roles in contagion as well. Thus, our results highlight the need for more research on the network effects in credit risk.

References

Acharya, V. V. and Yorulmazer, T. (2008). Information Contagion and Bank Herding. *Journal of Money, Credit and Banking*, 40(1):215–231.

Ahnert, T. and Georg, C.-P. (2018). Information Contagion and Systemic Risk. *Journal of Financial Stability*, 35:159–171.

Allen, F. and Gale, D. (2000). Financial Contagion. *Journal of Political Economy*, 108(1):1–33.

Augustin, P., Subrahmanyam, M. G., Tang, D. Y., and Wang, S. Q. (2014). Credit Default Swaps: A Survey. *Foundations and Trends in Finance*, 9(1-2):1–196.

Bharath, S. T. and Shumway, T. (2008). Forecasting Default with the Merton Distance to Default Model. *Review of Financial Studies*, 21(3):1339–1369.

Billio, M., Getmansky, M., Lo, A. W., and Pelizzon, L. (2012). Econometric Measures of Connectedness and Systemic Risk in the Finance and Insurance Sectors. *Journal of Financial Economics*, 104(3):535–559.

Blasques, F., Bräuning, F., and van Lelyveld, I. (2018). A Dynamic Stochastic Network Model of the Unsecured Interbank Lending Market. *Journal of Economic Dynamics & Control*, 90:310–342.

Brunnermeier, M., Clerc, L., Gabrieli, S., Kern, S., and Memmel, C. (2013). Assessing Contagion Risks from the CDS market. *ESRB Occasional Paper Series*, 4.

Caccioli, F., Shrestha, M., Moore, C., and Farmer, J. D. (2014). Stability Analysis of Financial Contagion due to Overlapping Portfolios. *Journal of Banking and Finance*, 46(1):233–245.

Campbell, J. Y. and Taksler, G. B. (2003). Equity Volatility and Corporate Bond Yields.

Cernov, M. and Urbano, T. (2018). Identification of EU Bank Business Models. *EBA Staff Paper Series*.

Cifuentes, R., Ferrucci, G., and Shin, H. S. (2005). Liquidity Risk and Contagion. *Journal of the European Economic Association*, 3:556–566.

Collin-Dufresne, P., Goldstein, R. S., and Martin, J. S. (2001). The Determinants of Credit Spread Changes. *Journal of Finance*, 56(6):2177–2207.

Cont, R. and Schaanning, E. (2018). Monitoring Indirect Contagion. *SSRN Electronic Journal*.

Coval, J. and Stafford, E. (2007). Asset Fire Sales (and Purchases) in Equity Markets. *Journal of Financial Economics*, 86(2):479–512.

Demirer, M., Diebold, F. X., Liu, L., and Yilmaz, K. (2018). Estimating Global Bank Network Connectedness. *Journal of Applied Econometrics*, 33(1):1–15.

Doucet, A., de Freitas, N., and Gordon, N. (2001). *Sequential Monte Carlo Methods in Practice*. Springer-Verlag New York.

Duarte, F. and Eisenbach, T. M. (2018). Fire-Sale Spillovers and Systemic Risk. *New York Fed Staff Reports*, 645.

Durbin, J. and Koopman, S. J. (2012). *Time Series Analysis by State Space Methods*. Oxford University Press.

Ericsson, J., Jacobs, K., and Oviedo, R. (2009). The Determinants of Credit Default Swap Premia. *Journal of Financial and Quantitative Analysis*, 44(1):109–132.

Fabbris, L. (1980). Measures of Predictor Variable Importance in Multiple Regression: an Additional Suggestion. *Quality and Quantity*, 14(6):787–792.

Fontana, A. and Scheicher, M. (2016). An Analysis of Euro Area Sovereign CDS and their Relation with Government Bonds. *Journal of Banking and Finance*, 62:126–140.

Genizi, A. (1993). Decomposition of R2 in Multiple Regression with Correlated Regressors. *Statistica Sinica*, 3:407–420.

Glasserman, P. and Peyton Young, H. (2015). How Likely is Contagion in Financial Networks? *Journal of Banking and Finance*, 54(642):383–399.

Greenwood, R., Landier, A., and Thesmar, D. (2015). Vulnerable Banks. *Journal of Financial Economics*, 115(3):471–485.

Grömping, U. (2015). Variable Importance in Regression Models. *WIREs Computational Statistics*, 7(2):137–152.

Grossman, S. J. and Stiglitz, J. E. (1980). On the Impossibility of Informationally Efficient Markets.

Hautsch, N., Schaumburg, J., and Schienle, M. (2015). Financial Network Systemic Risk Contributions. *Review of Finance*, 19(2):685–738.

Hommes, C. H. (2008). Bounded Rationality and Learning in Complex Markets. In Rosser, J. B. J., editor, *Handbook of Economic Complexity*. Edward Elgar, Cheltenham.

Kiewiet, G., van Lelyveld, I., and van Wijnbergen, S. (2017). Contingent Convertibles: Can the Market Handle Them? *CEPR Discussion Paper*, 12359.

Malik, S. and Pitt, M. K. (2011). Particle Filters for Continuous Likelihood Evaluation and Maximisation. *Journal of Econometrics*, 165(2):190–209.

Poledna, S., Martínez-Jaramillo, S., Caccioli, F., and Thurner, S. (2018). Quantification of Systemic Risk from Overlapping Portfolios in the Financial System. *arXiv*, 1802.00311.

Roengpitya, R., Tarashev, N., and Tsatsaronis, K. (2014). Bank Business Models. *BIS Quarterly Review*, 4:55–65.

Roengpitya, R., Tarashev, N., Tsatsaronis, K., and Villegas, A. (2017). Bank Business Models: Popularity and Performance. *BIS Working Papers*, 682.

Routledge, B. R. (1999). Adaptive Learning in Financial Markets. *The Review of Financial Studies*, 12:1165–1202.

Schön, T. B., Karlsson, R., and Gustafsson, F. (2006). The Marginalized Particle Filter in Practice. In *Aerospace Conference, 2006 IEEE*. IEEE.

Shleifer, A. and Vishny, R. W. (1992). Liquidation Values and Debt Capacity. *The Journal of Finance*, 47(4):1343–1366.

Wagener, W. (2010). Diversification at Financial Institutions and Systemic Crises. *Journal of Financial Intermediation*, 19:373–386.

Wang, D., Lelyveld, I. V., and Schaumburg, J. (2018). An Estimation Method for Spatial State-Space Models Based on the Smooth Marginalized Particle Filter. *mimeo*.

Zhang, B. Y., Zhou, H., and Zhu, H. (2009). Explaining Credit Default Swap Spreads with the Equity Volatility and Jump Risks of Individual Firms. *Review of Financial Studies*, 22(12):5099–5131.

Zuber, V. and Strimmer, K. (2011). High-dimensional Regression and Variable Selection Using CAR Scores. *Statistical Applications in Genetics & Molecular Biology*, 10(1):1–27.

7 Appendix

A Portfolio overlap measure

The statistical literature on relative importance and variable selection has proposed several methods for R^2 decomposition.[11] In multiple regression analysis, these methods help us understand how much explanatory power a regressor contributes in relation to all other regressors. Essentially, we are interested in how similar a particular bank's portfolio is to a stressed bank's portfolio, relative to the portfolios of all other banks. Translated into a variable selection problem, we are interested in the predictive power of a bank's portfolio regarding the stressed bank portfolio structure, compared to the remaining portfolios.

Algorithm 1 (Portfolio overlap measure)**.**
Let $y = bank_i$ be the $S \times 1$ regressand and $X = [bank_j]_{j \neq i}$ the $S \times (N-1)$ regressor matrix.

1. *Calculate $R_{XX} = \frac{1}{S} X^\top X$ and $R_{Xy} = \frac{1}{S} X^\top y$.*
2. *Estimate $c = R_{XX}^{-1/2} R_{Xy}$ where $R_{XX}^{1/2}$ denotes the matrix square root of R_{XX}.*
3. *Calculate raw overlap measure for all regressors $bank_j$ with $j \neq i$.*

$$\mu_{i,j}^* = \sum_{k=1}^{N-1} [R_{XX}]_{j,k}^2 c_k^2$$

4. *Set overlap measure between $bank_i$ and $bank_j$ to zero if they are disjoint.*

$$\mu_{i,j} = \begin{cases} \mu_{i,j}^* & \text{if } y^\top X_j \neq 0, \\ 0 & \text{otherwise.} \end{cases}$$

5. *Collect overlap measures in $1 \times (N-1)$ row vector and normalize with $\bar{\mu}_i = \sum_{k \neq i} \mu_{i,k}$.*

$$\mu_i = \frac{1}{\bar{\mu}_i} [\mu_{i,1}, \cdots, \mu_{i,N-1}].$$

A.1 Algorithm

Algorithm 1 details the steps to compute the portfolio overlap measure $\mu_{i,j}$. The basic idea is best illustrated in the context of a multiple regression of y on X: If the columns of X are mutually disjoint, then the R^2 of this regression is simply the sum of the R^2 of regressing y on each column of X, separately. However, this does not hold when the columns of X are not orthogonal. The idea is instead to use the nearest orthogonal matrix Z of X.[12] Since Z is orthogonal by definition, we can apply the same logic as before and regress y on Z, the orthogonal counterpart of X. However, this will give us the contributions of Z. Since were are interested in the contributions of X, the algorithm involves a further projection of X onto Z. For more details we refer to Zuber and Strimmer (2011).

[11] For a review of such methods we refer to Grömping (2015). Our measure is closest to Genizi (1993) as discussed in Zuber and Strimmer (2011).

[12] The closeness between two matrices is measured using the Forbenius norm. The matrix Z can be determined either using singular value decomposition (Fabbris, 1980) or by using the matrix square root (Genizi, 1993).

Figure 9: Hypothetical financial sector with six banks

Left: A hypothetical financial system with six banks and 40 assets. Each column represents a bank portfolio and the blue bars indicate the amount a banks holds of a certain asset. Right: The portfolio overlap matrix that results from applying Algorithm 1 to the asset holdings on the left panel. We can see that the resulting matrix is asymmetric and row-normalized.

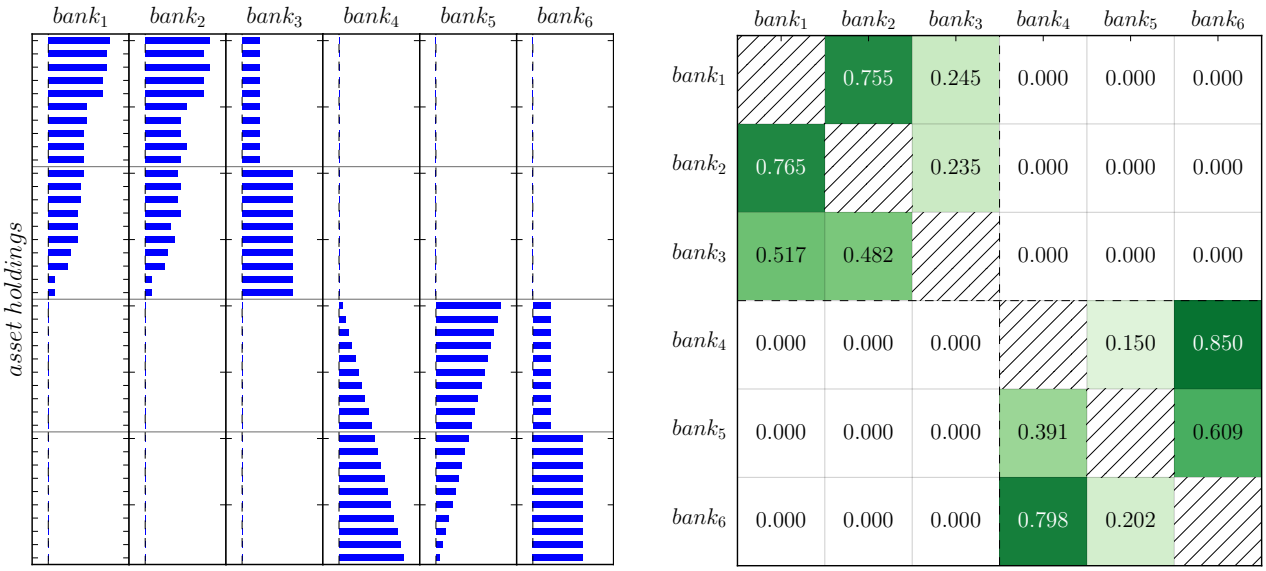

Figure 10: Visual representation of contagion process

This visualization depicts the contagion process of equation (5) for the portfolio overlap network of Figure 9. Each column represents one round of contagion. The assumed network intensity is $\rho = 0.7$.

(a) Chord diagram **(b) Contagion process**

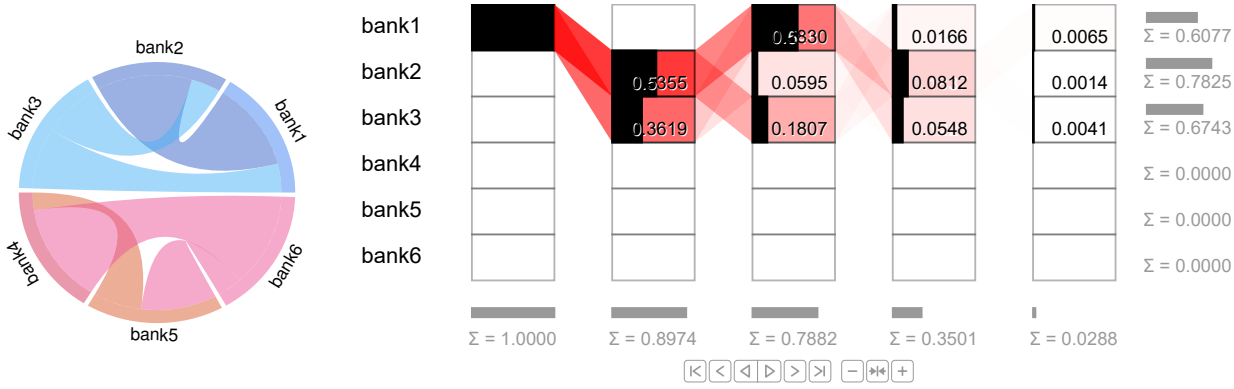

To obtain the portfolio overlap matrix W, we repeat Algorithm 1 as described in equation (1). The result for the hypothetical portfolios is presented in Figure 1 and 9, right panels. Note that the matrix satisfies all desired properties 1-3 and is by construction row-stochastic, i.e. each row adds up to one. This system is constructed to have three distinct features. First, the holdings of $bank_1$-$bank_3$ and $bank_4$-$bank_6$ form two disjoint groups. Second, the holdings of $bank_1$,$bank_2$ ($bank_4$,$bank_5$) are positively (negatively) correlated. Third, the holdings of $bank_3$ and $bank_6$ are randomly drawn: Their first halves follow $U[0, 10]$ while their second halves follow $U[10, 20]$.

We visualize this contagion process in Figure 10. Panel (a) is the graphical representation of the portfolio overlap network from Figure 9 while panel (b) demonstrates how a bank's demise spreads to its neighbors in an iterative fashion, according to the portfolio distances. With each round the network intensity decays geometrically. Panel (b) can also be viewed as the impulse response function of the network for a given shock.[13]

[13] An interactive visualization can be found at http://dieter.wang/contagionchain.

B Regression outputs of network models

Table 4: Regression results of network effects model

This table presents the regression coefficients of each country group (see Table 1). For confidentiality reasons, we present group averages. Note that the parentheses contain average p-values and therefore do not lend themselves for hypothesis testing. The bottom rows present the average R^2 coefficient of each group.

		Average	Country group				
Scope	Variable	All banks	BE,NL	ES	FR	AT,DE	IT
Europe	$eurostoxx50$	-0.5829	-0.4597	-0.3119	-1.1624	-0.4561	-0.6318
		(0.2246)	(0.2753)	(0.1823)	(0.0767)	(0.3269)	(0.1720)
	$slope^{EU}$	-0.0992	0.1544	-0.3479	-0.0165	-0.0266	-0.3854
		(0.3456)	(0.4133)	(0.2166)	(0.5475)	(0.3432)	(0.1639)
	$vstoxx$	0.0882	-0.1874	0.2678	0.0822	0.0612	0.2873
		(0.4408)	(0.2269)	(0.3486)	(0.4833)	(0.6826)	(0.2282)
	$L.eurostoxx50$	-0.2613	-0.0278	-0.1584	-0.5266	-0.4333	0.0456
		(0.4300)	(0.3930)	(0.7478)	(0.2022)	(0.3488)	(0.5490)
	$L.slope^{EU}$	-0.0235	-0.1387	-0.0557	0.1434	-0.0232	-0.0504
		(0.5279)	(0.5707)	(0.6906)	(0.4567)	(0.4409)	(0.5517)
	$L.vstoxx$	0.1767	0.1046	0.2836	0.0399	0.2312	0.1858
		(0.3909)	(0.2800)	(0.3433)	(0.5816)	(0.3860)	(0.3591)
Country	$bond10y^C$	0.0118	-0.1764	0.4389	-0.5010	-0.1917	0.8521
		(0.2888)	(0.4046)	(0.1895)	(0.2549)	(0.3700)	(0.1225)
	$eqidx^C$	-0.1495	-0.3879	-0.3710	0.5101	-0.3455	0.0418
		(0.3043)	(0.3205)	(0.5355)	(0.1404)	(0.2278)	(0.3716)
	$slope^C$	0.1646	0.1277	-0.0615	0.4684	0.3007	-0.2073
		(0.2279)	(0.3058)	(0.0848)	(0.2645)	(0.3262)	(0.0371)
	$L.bond10y^C$	-0.0219	0.2513	-0.3577	-0.2111	0.1372	-0.0574
		(0.4486)	(0.5811)	(0.4349)	(0.5468)	(0.2990)	(0.5084)
	$L.eqidx^C$	0.1806	-0.0691	0.0722	0.3167	0.4211	-0.0847
		(0.3687)	(0.5819)	(0.5257)	(0.1635)	(0.2593)	(0.4044)
	$L.slope^C$	0.0455	-0.1851	0.3599	0.2336	-0.1498	0.1389
		(0.4277)	(0.5910)	(0.4455)	(0.2386)	(0.4202)	(0.4562)
Bank	$const$	0.0482	0.0245	0.0681	0.0534	0.0244	0.1019
		(0.6089)	(0.7054)	(0.5755)	(0.4866)	(0.7606)	(0.3341)
	eq	-0.3242	-0.1819	-0.4611	-0.2576	-0.1389	-0.8523
		(0.3598)	(0.5388)	(0.0499)	(0.2411)	(0.6566)	(0.0000)
	lev	-0.0043	-0.0285	0.0550	0.0412	-0.0563	0.0094
		(0.4417)	(0.3636)	(0.2957)	(0.6670)	(0.3948)	(0.5500)
	$L.cds$	-0.2191	-0.0795	-0.2774	-0.0319	-0.5014	0.0818
		(0.2198)	(0.3669)	(0.2340)	(0.2318)	(0.1874)	(0.0643)
	$L.eq$	-0.1197	-0.0525	-0.0465	-0.1627	-0.1951	-0.0737
		(0.4237)	(0.7213)	(0.3047)	(0.2356)	(0.5427)	(0.1585)
R^2	Baseline	0.2839	0.2582	0.3072	0.2816	0.2232	0.4316
	NE, dirty	0.2886	0.2601	0.3105	0.2922	0.2279	0.4345
	NE, clean	0.4286	0.3311	0.4865	0.4015	0.3583	0.6814
	Observations	22	4	4	4	7	3

Table 5: Regression results of dynamic network effects model

This table presents the regression coefficients of each country group (see Table 1). For confidentiality reasons, we present group averages. Note that the parentheses contain average p-values and therefore do not lend themselves for hypothesis testing. The bottom rows present the average R^2 coefficient of each group.

		Average	Country group				
Scope	Variable	All banks	BE,NL	ES	FR	AT,DE	IT
Europe	$eurostoxx50$	-0.6284	-0.4899	-0.4160	-1.1646	-0.4491	-0.8000
		(0.1975)	(0.2398)	(0.2189)	(0.0689)	(0.2970)	(0.0519)
	$slope^{EU}$	-0.1516	0.1028	-0.3672	-0.1183	-0.0925	-0.3856
		(0.3429)	(0.4726)	(0.1825)	(0.4245)	(0.3991)	(0.1440)
	$vstoxx$	0.2554	0.0139	0.4314	0.2299	0.2293	0.4375
		(0.2604)	(0.1959)	(0.1523)	(0.3070)	(0.4237)	(0.0472)
	$L.eurostoxx50$	-0.2900	-0.0325	-0.1794	-0.5488	-0.4976	0.0486
		(0.4134)	(0.3546)	(0.7047)	(0.1954)	(0.3518)	(0.5382)
	$L.slope^{EU}$	-0.0805	-0.2040	-0.1138	0.0942	-0.0814	-0.1026
		(0.5291)	(0.5189)	(0.5856)	(0.5974)	(0.4716)	(0.5101)
	$L.vstoxx$	0.2125	0.1612	0.3235	0.0760	0.2535	0.2189
		(0.3489)	(0.3222)	(0.2904)	(0.5116)	(0.3396)	(0.2671)
Country	$bond10y^C$	0.1521	-0.0262	0.5171	-0.2798	-0.0073	0.8512
		(0.3467)	(0.2769)	(0.2666)	(0.4624)	(0.4278)	(0.2030)
	$eqidx^C$	-0.1429	-0.3251	-0.3235	0.4709	-0.3704	0.0531
		(0.3723)	(0.5180)	(0.5758)	(0.1662)	(0.2326)	(0.5076)
	$slope^C$	0.0660	0.0305	-0.1145	0.3325	0.1667	-0.2364
		(0.2257)	(0.2150)	(0.0858)	(0.2306)	(0.3776)	(0.0657)
	$L.bond10y^C$	0.0167	0.2845	-0.2801	-0.1953	0.1824	-0.0488
		(0.4170)	(0.4877)	(0.3794)	(0.5608)	(0.2865)	(0.4854)
	$L.eqidx^C$	0.1690	-0.0914	0.0427	0.3151	0.4346	-0.1302
		(0.3703)	(0.5174)	(0.5297)	(0.1547)	(0.2616)	(0.5027)
	$L.slope^C$	0.0461	-0.1734	0.3328	0.2375	-0.1511	0.1610
		(0.4120)	(0.5948)	(0.3753)	(0.2452)	(0.4112)	(0.4414)
Bank	$const$	0.0557	0.0294	0.0890	0.0541	0.0295	0.1098
		(0.5787)	(0.7319)	(0.4744)	(0.4850)	(0.7341)	(0.2757)
	eq	-0.2662	-0.1420	-0.4418	-0.2369	-0.0854	-0.6586
		(0.3442)	(0.5538)	(0.0618)	(0.3032)	(0.5568)	(0.0000)
	lev	0.0007	-0.0131	0.0397	0.0482	-0.0475	0.0161
		(0.4569)	(0.4205)	(0.2478)	(0.7308)	(0.3767)	(0.6060)
	$L.cds$	-0.2625	-0.1342	-0.3497	-0.0502	-0.5274	0.0175
		(0.2440)	(0.3722)	(0.2416)	(0.2059)	(0.1835)	(0.2685)
	$L.eq$	-0.1421	-0.0959	-0.0704	-0.1815	-0.1987	-0.1150
		(0.3719)	(0.5428)	(0.3013)	(0.2331)	(0.5203)	(0.0768)
R^2	Baseline	0.2839	0.2582	0.3072	0.2816	0.2232	0.4316
	DNE, dirty	0.2966	0.2726	0.3161	0.2993	0.2337	0.4456
	DNE, clean	0.4302	0.3142	0.4988	0.3885	0.3649	0.7016
	Observations	22	4	4	4	7	3

C Residual diagnostics

Figure 11: Residual tests

(a) Average correlations of residuals and squared residuals

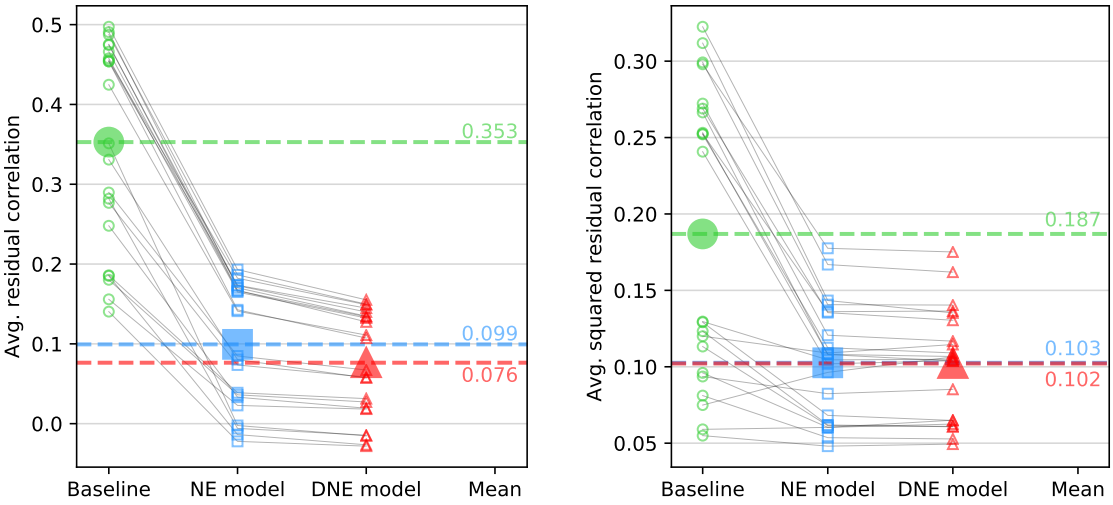

(b) Ljung-Box test for residual autocorrelation (p-values)

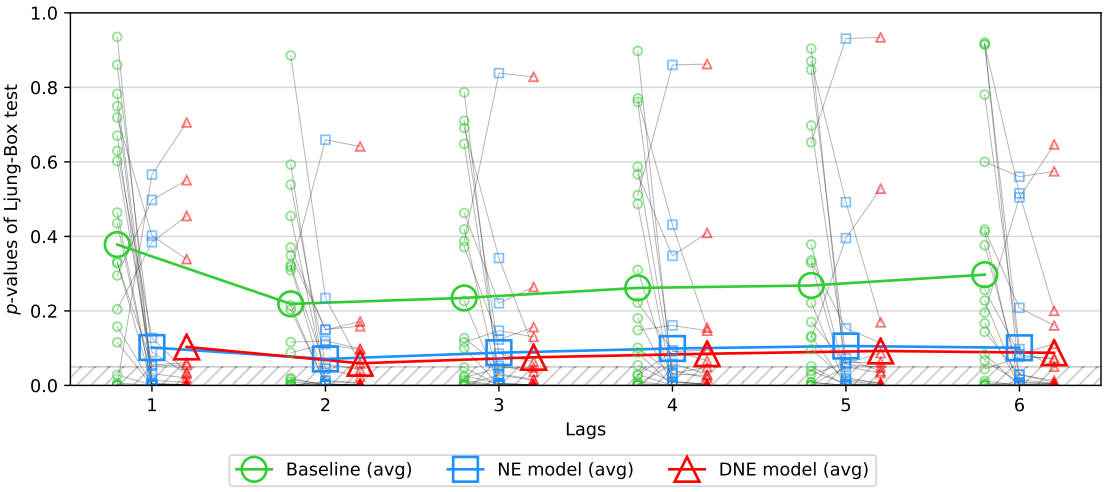

(c) ARCH-LM test for residual heteroskedasticty (p-values)